bioRxiv preprint doi: https://doi.org/10.1101/083436; this version posted October 25, 2016. The copyright holder for this preprint (which was not certified by peer review) is the author/funder, who has granted bioRxiv a license to display the preprint in perpetuity. It is made available under aCC-BY-NC-ND 4.0 International license.

UNC-5 (UNC5) Regulates the Length and Number of Processes that *Caenorhabditis elegans* Neurons Can Develop

Gerard Limerick[*, †], Xia Tang[*, †], Won Suk Lee[*, †], Ahmed Mohamed[*], Aseel Al-Aamiri[*], and William G. Wadsworth[*]

[*]Department of Pathology and Laboratory Medicine, Rutgers Robert Wood Johnson Medical School, Piscataway, NJ 08854

†These authors contributed equally to this work

bioRxiv preprint doi: https://doi.org/10.1101/083436; this version posted October 25, 2016. The copyright holder for this preprint (which was not certified by peer review) is the author/funder, who has granted bioRxiv a license to display the preprint in perpetuity. It is made available under aCC-BY-NC-ND 4.0 International license.

12 running title: neuronal outgrowth patterning

13

14 key words: neuronal development, axon guidance, asymmetric localization, *Caenorhabditis*

15 *elegans*, netrin and wnt signaling

16

17 corresponding author:

18 William G. Wadsworth

19 Department of Pathology and Laboratory Medicine

20 Rutgers Robert Wood Johnson Medical School

21 675 Hoes Lane West

22 Piscataway, NJ 08854-5635

23 732-235-5768

24 william.wadsworth@rwjms.rutgers.edu

bioRxiv preprint doi: https://doi.org/10.1101/083436; this version posted October 25, 2016. The copyright holder for this preprint (which was not certified by peer review) is the author/funder, who has granted bioRxiv a license to display the preprint in perpetuity. It is made available under aCC-BY-NC-ND 4.0 International license.

Abstract

Neurons extend processes that vary in number, length, and direction of outgrowth. Extracellular molecules act as cues to regulate this patterning. In *Caenorhabditis elegans,* neurons respond to the UNC-6 (netrin) cue via UNC-5 (UNC5) and UNC-40 (DCC) receptors. Here we present evidence that UNC-5 regulates the length and number of processes that neurons develop. Genetic analysis suggests UNC-5 functions with UNC-6 and EGL-20 (wnt), the SAX-3 (Robo) receptor, and the cytoplasmic proteins UNC-53 (NAV2), MIG-15 (NIK kinase), and MADD-2 (TRIM) to regulate the asymmetric localization of UNC-40 to a surface of the neuron. We have postulated that UNC-40 polarization is self-organizing and that the surface to which UNC-40 localizes and mediates outgrowth is stochastically determined. At any instance of time, there is a probability that UNC-40-mediated outgrowth will occur in a specific direction. We find that UNC-5 activity reduces the degree to which the direction of outgrowth fluctuations over time. Random walk modeling predicts that by decreasing the fluctuation UNC-5 activity increases the mean-squared distance that outgrowth movement could covered over a given time. This suggests that UNC-5 activity creates outgrowth patterns by varying the rate of outgrowth along a surface of the neuron.

bioRxiv preprint doi: https://doi.org/10.1101/083436; this version posted October 25, 2016. The copyright holder for this preprint (which was not certified by peer review) is the author/funder, who has granted bioRxiv a license to display the preprint in perpetuity. It is made available under aCC-BY-NC-ND 4.0 International license.

Introduction

During development, an intricate network of neuronal connections is established. As processes extend from the cell bodies of neurons distinct patterns of outgrowth emerge. Some extensions remain as a single process, whereas others branch and form multiple processes. If they branch, the extensions can travel in the same or in different directions. Processes vary in length. Extracellular cues are known to influence this patterning, but the underlying logic that govern the formation of patterns remains a mystery.

The secreted extracellular UNC-6 (netrin) molecule and its receptors, UNC-5 (UNC5) and UNC-40 (DCC) are highly conserved in invertebrates and vertebrates, and are known to play key roles in cell and axon migrations. In *Caenorhabditis elegans*, UNC-6 is produced by ventral cells and is thought to form a gradient with its highest concentration around the ventral midline (WADSWORTH *et al.* 1996; WADSWORTH AND HEDGECOCK 1996; ASAKURA *et al.* 2007). It's been observed that neurons that express the receptor UNC-40 (DCC) extend axons ventrally, towards the UNC-6 sources; whereas neurons that express the receptor UNC-5 (UNC5) alone or in combination with UNC-40 extend axons dorsally, away from the UNC-6 sources (HEDGECOCK *et al.* 1990; LEUNG-HAGESTEIJN *et al.* 1992; CHAN *et al.* 1996; WADSWORTH *et al.* 1996).

It is thought that the function of UNC-5 (UNC5) in axon development is to mediate a repulsive response by the neuron to UNC-6 (netrin) (LEUNG-HAGESTEIJN *et al.* 1992; HONG *et al.* 1999; KELEMAN AND DICKSON 2001; MOORE *et al.* 2007). This drives outgrowth away from the UNC-6 (netrin) sources. However recent studies suggest that UNC-5 in *C. elegans* also plays a role in orienting outgrowth towards, and perpendicular, to the UNC-6 source. For

bioRxiv preprint doi: https://doi.org/10.1101/083436; this version posted October 25, 2016. The copyright holder for this preprint (which was not certified by peer review) is the author/funder, who has granted bioRxiv a license to display the preprint in perpetuity. It is made available under aCC-BY-NC-ND 4.0 International license.

example, a synergistic interaction between UNC-5 and EGL-20 has been suggested for the guidance of AVM and PVM axons towards the UNC-6 source. In either *unc-5* or *egl-20* mutants the ventral extension of AVM and PVM axons is only slightly impaired, whereas in the double mutants there is a much greater penetrance (LEVY-STRUMPF AND CULOTTI 2014). EGL-20 (Wnt) is a secreted cue expressed from posterior sources (PAN *et al.* 2006). In the HSN neuron, both UNC-5 and EGL-20 affect to which surface the UNC-40 receptor will localize and, correspondingly, they affect the direction of HSN extension (KULKARNI *et al.* 2013). Finally, in different genetic backgrounds UNC-5 has been observed to affect outgrowth along the anterior-posterior directions (LEVY-STRUMPF AND CULOTTI 2007; WATARI-GOSHIMA *et al.* 2007; LEVY-STRUMPF AND CULOTTI 2014; LEVY-STRUMPF *et al.* 2015; BHAT AND HUTTER 2016).

UNC-5 activity has also been implicated in axon branching and length of extension. We previously reported that loss of UNC-5 function, or of the receptor SAX-3 (Robo), suppresses branch formation that is induced by the expression of the N-terminal fragment of UNC-6, UNC-6ΔC (LIM *et al.* 1999). A characteristic of the response that a neuron has to UNC-6ΔC is that additional processes arise which are still guided by UNC-6ΔC (LIM *et al.* 1999). In other words, UNC-6ΔC can trigger the formation of additional processes from a neuron without seriously compromising the guidance response that the neuron has to UNC-6ΔC. A screen for mutations that suppress this patterning activity revealed that intercellular signaling pathways regulate the ability of UNC-6ΔC to form new extension patterns (WANG AND WADSWORTH 2002). This observation indicates that the additional processes arise because the neuron's response to UNC-6ΔC internally patterns new sites of outgrowth extension. UNC-5 and SAX-3 appear to regulate this signaling. In addition, we reported that the overextension of the PLM axon which occurs in *rpm-1* mutants can be suppressed

bioRxiv preprint doi: https://doi.org/10.1101/083436; this version posted October 25, 2016. The copyright holder for this preprint (which was not certified by peer review) is the author/funder, who has granted bioRxiv a license to display the preprint in perpetuity. It is made available under aCC-BY-NC-ND 4.0 International license.

by loss of SAX-3 or UNC-5 function (Li *et al.* 2008). These branching and extension phenotypes are difficult to reconcile with the notion that the role of UNC-5 is simply to mediate repulsion away from UNC-6 sources, and they suggest that our understanding of UNC-5 function is incomplete.

In this paper, we show that UNC-5 regulates the length and number of extensions that neurons can form. We further present evidence indicating that UNC-5 (UNC5) functions together with UNC-6 (netrin) and EGL-20 (wnt), the SAX-3 (Robo) receptor, and the UNC-53 (NAV2), MIG-15 (NIK kinase), and MADD-2 (TRIM) cytoplasmic proteins to regulate UNC-40 asymmetric localization at a surface of the HSN neuron. Finally, we discuss how UNC-5 could control the length and number of extensions by regulating the asymmetric localization of UNC-40.

bioRxiv preprint doi: https://doi.org/10.1101/083436; this version posted October 25, 2016. The copyright holder for this preprint (which was not certified by peer review) is the author/funder, who has granted bioRxiv a license to display the preprint in perpetuity. It is made available under aCC-BY-NC-ND 4.0 International license.

Materials and Methods

Strains

Strains were handled at 20 ℃ by using standard methods (Brenner, 1974) unless stated otherwise. A Bristol strain N2 was used as wild type. The following alleles were used: **LGI**, *unc-40(e1430), unc-40(ur304), zdIs5[mec-4::GFP]*; **LGII**, *unc-53(n152)*; **LGIV,** *unc-5(e152), unc-5(e53), unc-5(ev480), unc-5(ev585),egl-20(n585), kyIs262[unc-86::myr-GFP;odr-1::dsRed];* **LGIV,** *madd-2(ky592), madd-2(tr103)*; **LGX**, *mig-15(rh148), unc-6(ev400)*, *sax-3(ky123), sax-3(ky200).*

Transgenes maintained as extrachromosomal arrays included: *kyEx1212 [unc-86::unc-40-GFP;odr-1::dsRed].*

Analysis of axon outgrowth and cell body position

HSN neurons were visualized using expression of the transgene *kyIs262[unc-86::myr-GFP].* The mechanosensory neurons, AVM, ALM, and PLM, were visualized using the expression of the transgene *zdIs5[Pmec-4::GFP]*. Synchronized worms were obtained by allowing eggs to hatch overnight in M9 buffer without food. The larval stage was determined by using differential interference contrast (DIC) microscopy to examine the gonad cell number and gonad size. Staged nematodes larvae were mounted on a 5% agarose pad with 10 mM levamisole buffer. Images were taken using epifluorescent microscopy with a Zeiss 63X water immersion objective.

The number of process during early L1 larval stage was scored by counting the number of processes that extended for a distance greater than the length of one cell body. We report whether there were no such processes, one process or more than one processes. In the L2 larval stage, a single early process was scored if there was only one major extension from

bioRxiv preprint doi: https://doi.org/10.1101/083436; this version posted October 25, 2016. The copyright holder for this preprint (which was not certified by peer review) is the author/funder, who has granted bioRxiv a license to display the preprint in perpetuity. It is made available under aCC-BY-NC-ND 4.0 International license.

the ventral leading edge. The HSN cell body in L2 stage larvae was scored as dorsal if the cell body had failed to migrate ventrally and was not positioned near the PLM axon. In L4 stage larvae, a multiple ventral processes phenotype was scored if more than one major extension protruded from the ventral side of cell body.

Extension into the nerve ring was scored as defective if the axon did not extend further than approximately half the width of the nerve ring. Anterior extension was scored as defective if the axon did not extend further anteriorly than the nerve ring. PLM axons are scored as over-extending if they extended further anterior than the position of the ALM cell body.

Analysis of the direction of HSN outgrowth

HSN was visualized using the transgene *kyIs262[unc-86::myr-GFP].* L4 stage larvae were mounted on a 5% agarose pad with 10 mM levamisole buffer. An anterior protrusion was scored if the axon extended from the anterior side of the cell body for a distance greater than the length of three cell bodies. A dorsal or posterior protrusion was scored if the axon extended dorsally or posteriorly for a distance greater than two cell body lengths. The HSN was considered multipolar if more than one process extended a length greater than one cell body. Images were taken using epifluorescent microscopy with a Zeiss 40X objective.

Analysis of the UNC-40::GFP localization in L2 stage animal

For analysis of UNC-40::GFP localization, L2 stage larvae with the transgenic marker *kyEx1212[unc-86::unc-40::GFP; odr-1::dsRed]* were mounted on a 5% agarose pad with 10 mM levamisole buffer. Staging was determined by examining the gonad cell number and gonad size under differential interference contrast (DIC) microscopy. Images were taken using epifluorescent microscopy with a Zeiss 63X water immersion objective. The UNC-

bioRxiv preprint doi: https://doi.org/10.1101/083436; this version posted October 25, 2016. The copyright holder for this preprint (which was not certified by peer review) is the author/funder, who has granted bioRxiv a license to display the preprint in perpetuity. It is made available under aCC-BY-NC-ND 4.0 International license.

40::GFP localization was determined by measuring the average intensity under lines drawn along the dorsal and ventral edges of each HSN cell body by using ImageJ software. For analysis of the anterior–posterior orientation of UNC-40::GFP, the dorsal segment was geometrically divided into three equal lengths (dorsal anterior, dorsal central and dorsal posterior segments). The line-scan intensity plots of each of these segments were recorded. ANOVA test was used to determine if there is a significant difference between intensities of three segments. The dorsal distribution was considered uniform if $p \geq 0.05$ and was considered asymmetrical if $p \leq 0.05$. Within an asymmetric population, the highest percent intensity was considered to localize UNC-40::GFP to either anterior, posterior or central domain of the dorsal surface.

Computations

A program to simulate a two-dimensional lattice random walk based on the probability of dorsal, ventral, anterior, and posterior outgrowth for a mutant (Table 1) was created using MATLAB. (The directions of the axons from multipolar neurons were not scored. These axons appear to behave the same as the axons from monopolar neurons, but this has not yet been tested.) The probability of dorsal, ventral, anterior, or posterior outgrowth was assigned for the direction of each step of a random walk moving up, down, left or right, respectively. Each variable is considered independent and identically distributed. Simulations of 500 equal size steps (size =1) were plotted for 50 tracks (Figure 1B and Figure 4 inserts). A Gaussian distribution for the final positions of the tracks was generated using Matlab's randn function (Figure 4).

bioRxiv preprint doi: https://doi.org/10.1101/083436; this version posted October 25, 2016. The copyright holder for this preprint (which was not certified by peer review) is the author/funder, who has granted bioRxiv a license to display the preprint in perpetuity. It is made available under aCC-BY-NC-ND 4.0 International license.

The mean squared displacement (MSD) is used to provide a quantitative characteristic of the motion that would be created by the outgrowth activity undergoing the random walk. Using the random walks generated for a mutant the MSD can be calculated:

$$msd(\tau) = < [r(t+\tau) - \mathrm{r}(t)]^2 >$$

Here, r(*t*) is the position at time *t* and τ is the lag time between two positions used to calculate the displacement, Δr(τ) = r(*t*+τ) - r(*t*). The time-average over *t* and the ensemble-average over the 50 trajectories were calculated. This yields the MSD as a function of the lag time. A coefficient giving the relative rate of diffusion was derived from a linear fit of the curve. The first two lag time points were not considered as the paths often approximate a straight line at short intervals.

bioRxiv preprint doi: https://doi.org/10.1101/083436; this version posted October 25, 2016. The copyright holder for this preprint (which was not certified by peer review) is the author/funder, who has granted bioRxiv a license to display the preprint in perpetuity. It is made available under aCC-BY-NC-ND 4.0 International license.

Results

UNC-5 regulates the pattern of outgrowth from the HSN neuron

The HSN neuron is used to study how a neuron responds to extracellular guidance cues. The HSN neuron sends a single axon to the ventral nerve cord, which is a source of the UNC-6 cue (WADSWORTH *et al.* 1996; ADLER *et al.* 2006; ASAKURA *et al.* 2007). The formation of the axon is dynamic (ADLER *et al.* 2006). Shortly after hatching HSN extends short neurites in different directions. These neurites, which dynamically extend and retract filopodia, become restricted to the ventral side of the neuron where a leading edge forms. Multiple neurites extend from this surface until one develops into a single axon extending to the ventral nerve cord. Extracellular GFP-tagged UNC-40 is observed to asymmetrically localize ("cluster") at the ventral side of HSN as the ventral leading edge forms (ADLER *et al.* 2006; XU *et al.* 2009; KULKARNI *et al.* 2013). UNC-40 receptor localization within the plasma membrane can regulate the actin cytoskeleton. UNC-40, as well as the SAX-3 (Robo) and VAB-1 (Eph) receptors, has been shown to polarize the distribution of F-actin in cells (BERNADSKAYA *et al.* 2012). Reflecting the dynamic morphological changes that occurs as the HSN axon forms, the site of asymmetric UNC-40::GFP localization fluctuates in the neurites and along the ventral surface of the neuron (KULKARNI *et al.* 2013). Measurements of growth cone size, maximal length, and duration of growth cone filopodia indicate that UNC-6, UNC-40, and UNC-5 control the dynamics of protrusion (NORRIS AND LUNDQUIST 2011).

We observe that in *unc-5* mutants, the patterns of extension are altered. In wild-type animals at the L1 stage of development most HSN neurons extends more than one short neurite, however in *unc-5(e53)* mutants nearly half the neurons do not extend a process (Figures 1A and 1B). Further, we find that *sax-3* is required for this suppression as most

bioRxiv preprint doi: https://doi.org/10.1101/083436; this version posted October 25, 2016. The copyright holder for this preprint (which was not certified by peer review) is the author/funder, who has granted bioRxiv a license to display the preprint in perpetuity. It is made available under aCC-BY-NC-ND 4.0 International license.

211 neurons will extend in *unc-5(e53);sax-3(ky200)* mutants. During the L2 stage in wild-type
212 animals a prominent ventral leading edge forms and the cell body undergoes a short ventral
213 migration that is completed by the L3 stage, however in *unc-5* mutants a single large ventral
214 process may form early during the L2 stage and the cell body may fail to migrate (Figures
215 1A, 1C and 1E). It may be that the ventral migration of the HSN cell body requires the
216 development of a large leading edge with multiple extensions. Together the observations
217 indicate that loss of *unc-5* function affects the patterning of outgrowth, *i.e.* the timing, length,
218 and number of extensions that form. Loss of *unc-5* function does not prevent movement, in
219 fact, a single large ventral extension can form in the mutant at a time that is even earlier
220 than when a single ventral extension can be observed in wildtype.

221

222 We tested four different *unc-5* alleles in these experiments. The *unc-5(e53)* allele is a
223 putative molecular null allele, *unc-5(e480)* is predicted to truncate UNC-5 after the
224 cytoplasmic ZU-5 domain and before the Death Domain, *unc-5(e152)* is predicted to
225 truncate UNC-5 before the ZU-5 domain and Death Domain, and *unc-5(ev585)* is a
226 missense allele that affects a predicted disulfide bond in the extracellular Ig(C) domain
227 (KILLEEN *et al.* 2002). Although both the *unc-5(e480)* and *unc-5(e152)* are predicted to
228 cause premature termination of protein translation in the cytodomain, the *unc-5(e152)*
229 retains the signaling activity that prevents these phenotypes. Based on other phenotypes,
230 previous studies reported that the *unc-5(e152)* allele retains UNC-40-dependent signaling
231 functions (MERZ *et al.* 2001; KILLEEN *et al.* 2002).

232

233 **UNC-5 is required for the induction of multiple HSN axons by UNC-6ΔC and a *mig-15***
234 **mutation**

bioRxiv preprint doi: https://doi.org/10.1101/083436; this version posted October 25, 2016. The copyright holder for this preprint (which was not certified by peer review) is the author/funder, who has granted bioRxiv a license to display the preprint in perpetuity. It is made available under aCC-BY-NC-ND 4.0 International license.

The results above suggest that UNC-5 activity can regulate the number of HSN extensions that will form. Previously we reported that expression of the N-terminal fragment of UNC-6, UNC-6ΔC, induces excessive branching of ventral nerve cord motor neurons and that UNC-5 can suppress this branching (LIM *et al.* 1999). We now report that HSN develops an extra process in response to UNC-6ΔC and that UNC-5 suppresses the development of the extra process (Figures 1D and 1F). Because HSN processes are guided ventrally by UNC-6ΔC even when UNC-5 is not present, UNC-5 does not alter HSN axon guidance. Further, because loss of UNC-5 function reduces the number of HSN processes that form and genetic data suggests that UNC-6ΔC induces additional processes by altering intracellular signaling (WANG AND WADSWORTH 2002), we surmise that UNC-5 signaling plays a cell-autonomous role within HSN to regulate intracellular signaling that affects branching. In support of suppression though cell-autonomous signaling, we also find that the UNC-6ΔC phenotype is suppressed by *mig-10(ct141)* (Figures 1F). MIG-10 (lamellipodin) is a cytoplasmic adaptor protein that promotes HSN extensions (CHANG *et al.* 2006; QUINN *et al.* 2006).

We find that a *mig-15* mutation also causes extra HSN processes and that the loss of UNC-5 function suppresses the extra HSN processes (Figures 1F and 1G). MIG-15 (NIK kinase) is cytoplasmic protein and evidence indicates that *mig-15* functions cell-autonomously to mediate a response to UNC-6 (POINAT *et al.* 2002; TEULIÈRE *et al.* 2011). It's been proposed that *mig-15* acts in the same pathway as *unc-5* to polarize the growth cone in response to the UNC-6 (TEULIÈRE *et al.* 2011). Mutations in *mig-15* are known to affect axon development, as well as Q neuroblast polarity and migration (POINAT *et al.* 2002; SHAKIR *et al.* 2006; TEULIÈRE *et al.* 2011; YANG *et al.* 2014). MIG-15 regulates the intracellular localization of UNC-40 in HSN (YANG *et al.* 2014). In our experiments we used the *mig-*

bioRxiv preprint doi: https://doi.org/10.1101/083436; this version posted October 25, 2016. The copyright holder for this preprint (which was not certified by peer review) is the author/funder, who has granted bioRxiv a license to display the preprint in perpetuity. It is made available under aCC-BY-NC-ND 4.0 International license.

15(rh148) allele, which causes a missense mutation in the ATP-binding pocket of the kinase domain and is a weak allele of *mig-15* (SHAKIR *et al.* 2006; CHAPMAN *et al.* 2008).

UNC-5 is required for ALM and AVM branching and extension, and for PLM overextension

The *mig-15* results suggest that altering *mig-15* function creates a sensitized genetic background. That is, the *unc-5(ev480)* mutation suppresses HSN outgrowth extension in both the wild-type and *mig-15(rh148)* backgrounds, but the *mig-15* mutation creates a stronger patterning phenotype. We examined whether UNC-5 might affect the outgrowth patterning of other neurons in the *mig-15* mutants. We examined the patterning of the ALM and AVM extensions at the nerve ring and found that genetic interactions involving *unc-5, unc-40,* and *mig-15* affect outgrowth patterning (Figures 2A, 2B, and 2C). The AVM axon in *mig-15(rh148);unc-5(e53)* mutants often fails to extend anteriorly from the branch point and only extends into the nerve ring, or it fails to extend into the nerve ring and only extends anteriorly, or it fails to do both and terminates at this point. The axon often fails to branch into the nerve ring in *unc-40(e1430)* mutants, although it extends anteriorly. By comparison, in *unc-40(e1430);mig-15(rh148)* mutants more axons extend into the nerve ring, but fewer extend anteriorly.

It was previously reported that in *rpm-1* mutants the PLM axon will overextend in the anterior direction and that this phenotype can be suppressed by *sax-3* and *unc-5* mutations (LI *et al.* 2008).

This indicates that UNC-5 can also suppress outgrowth in the anterior direction, which is perpendicular to the ventral UNC-6 sources. We now observe that in *mig-15(rh148)*

bioRxiv preprint doi: https://doi.org/10.1101/083436; this version posted October 25, 2016. The copyright holder for this preprint (which was not certified by peer review) is the author/funder, who has granted bioRxiv a license to display the preprint in perpetuity. It is made available under aCC-BY-NC-ND 4.0 International license.

mutants the PLM axon also often fails to terminate at its normal position and instead extends beyond the ALM cell body. This overextension is suppressed in *unc-5(e53);mig-15(rh148)* and *unc-40(e1430);mig-15(rh148)* mutants (Figures 2D and 2E). In summary, the HSN, AVM, ALM, and PLM experiments show that the spatial extent of movement is altered by UNC-5 activity. This function is not dependent on the direction of outgrowth relative to the UNC-6 sources.

***unc-5* acts with other genes to control the probability of HSN extension in each direction**

We have observed that in certain mutants the direction of outgrowth from the HSN cell body can vary (XU *et al.* 2009; KULKARNI *et al.* 2013; TANG AND WADSWORTH 2014; YANG *et al.* 2014). The different directions from which the axon projects from the HSN cell body can be scored to create a probability distribution for the direction of movement. The probability distribution gives an approximation of how much the direction of outgrowth fluctuates. To understand how the fluctuation could affect outgrowth movement, a random walk model is used. Random walks describe movement that occurs as a series of steps in which the angles and the distances between each step is decided according to some probability distribution. By using the probability distribution obtained from a mutant for each step of a random walk, and by keeping the distance of each step equal, a random walk can be constructed (Figure 3A). In effect, this method applies the probability distribution to discrete particles having idealized random walk movement on a lattice. By plotting random walks derived from wild-type animals and different mutants, the relative effect that mutations have on random walk movement can be visualized. For example, Figure 1B shows 50 tracks of 500 steps for wild type and two mutants (mutant A is *unc-5(e53)* and mutant B is *egl-20(n585);sax-3(ky123)*). One property of movement that this method can reveal is the effect

bioRxiv preprint doi: https://doi.org/10.1101/083436; this version posted October 25, 2016. The copyright holder for this preprint (which was not certified by peer review) is the author/funder, who has granted bioRxiv a license to display the preprint in perpetuity. It is made available under aCC-BY-NC-ND 4.0 International license.

that a mutation has on the displacement of movement. After 500 steps the displacement from the origin (0,0) is on average less for mutant A than for wild type, and less for mutant B than for wild type or mutant A. In an extending neuron, mass (the molecular species) are sustained at the leading edge. The assay compares the effect that different mutations would have on the movement of mass at the leading edge of an extension if the conditions of the system were kept constant. Of course, *in vivo* the conditions are not constant. For one, as an extension moves it will encounter new environments where the cues may be new or at different concentrations, all of which affect the probability distribution. As such, the graphs do not predict the actual movements of migrating axons, but rather show the relative effect that a mutation has on the movement of outgrowth.

For different strains, we score whether the HSN axon forms in the dorsal, anterior, posterior, or ventral direction (Table 1). Using our assay, we compared the effects that a mutation has on the properties of movement. In wild-type animals, there is a high probability for outgrowth in the ventral direction. The analysis shows that conditions in wild-type create nearly straight-line movement, *i.e.* if the same random walk is repeatedly done for the same number of steps, starting at the same origin, the final position of the walk along the x axis does not vary too much. In comparison, we find that a mutation can create random walk movement in which the final position is more varied. This variation occurs because the mutation increases the probability of outgrowth in other directions during axon formation. For each mutation, we simulate 50 random walks of 500 steps and derive the mean and standard deviation of the final position along the X axis. To compare strains, we plot the normal distribution, setting the mean at the same value for each. The difference between the curve for a mutant and wild type shows the degree to which the mutation caused the direction of outgrowth to fluctuate.

bioRxiv preprint doi: https://doi.org/10.1101/083436; this version posted October 25, 2016. The copyright holder for this preprint (which was not certified by peer review) is the author/funder, who has granted bioRxiv a license to display the preprint in perpetuity. It is made available under aCC-BY-NC-ND 4.0 International license.

The results reveal three different distribution patterns (Figure 4). One class is the wild-type distribution, which has the distribution curve with the highest peak. The second class comprises *unc-5, egl-20, unc-53,* and *unc-6* in which the distribution curve is flatter than the wild-type curve. The third class has the flattest distribution curve and comprises the double combinations of *unc-5, egl-20, unc-53,* and *unc-6* as well as *madd-2, sax-3,* and *mig-15*. This class indicates the greatest degree of fluctuation. Loss of both *unc-6* and *egl-20* function causes this state, as well as loss of *unc-6* and *unc-5,* or *egl-20* and *unc-5.* The ability to cause the direction of movement to fluctuate is not associated with a specific direction of advection. For example, *unc-5;sax-3, unc-53;unc-6, unc-40;egl-20,* and *madd-2;sax-3* each show a widely dispersed pattern but the direction is ventral, dorsal, anterior, and posterior, respectively.

Mean squared displacement (MSD) is a measurement of the spatial extent of random motion. The MSD can be calculated from the random walk data. Plotting MSD as a function of the time interval shows how much an object displaces, on average, in a given interval of time, squared (Figure 5A). The results show that loss of UNC-6, UNC-5, or UNC-40 alters the MSD. For normal molecular diffusion the slope of the MSD curve is directly related to the diffusion coefficient. In cell migration models this value is referred to as the random motility coefficient. Coefficients are experimentally determined; they describe how long it takes a particular substance to move through a particular medium. We determine this value in order to numerically compare how the mutations can alter displacement relative to wild type (Figure 5B). The value is reduced in *unc-5, egl-20, unc-53,* and *unc-6* mutants, but not as much as in the other mutants, including those with double mutations.

bioRxiv preprint doi: https://doi.org/10.1101/083436; this version posted October 25, 2016. The copyright holder for this preprint (which was not certified by peer review) is the author/funder, who has granted bioRxiv a license to display the preprint in perpetuity. It is made available under aCC-BY-NC-ND 4.0 International license.

359 **_unc-5_ acts with other genes to control the probability of asymmetric UNC-40 receptor**
360 **localization at each side of the HSN neuron**

361 UNC-40::GFP becomes localized to the ventral side of HSN beginning in the early L2 stage,
362 whereas in *unc-6* loss-of-function mutants UNC-40::GFP is uniformly dispersed around the
363 periphery of HSN (ADLER *et al.* 2006; KULKARNI *et al.* 2013). In *unc-53(n152); unc-5(e53)*
364 mutants UNC-40::GFP localization is similar to that observed in *unc-6(ev400)* or *unc-5(e53);*
365 *unc-6(ev400)* mutants, *i.e.* asymmetric UNC-40::GFP localization in not observed. In both
366 *unc-53(n152)* and *unc-5(e53)* mutants UNC-40::GFP is asymmetrically localized, however
367 there is a higher probability that the localization occurs at surfaces other than at the ventral
368 surface (KULKARNI *et al.* 2013). These results show that there are genetic interactions
369 among *unc-5*, *unc-6*, and *unc-53* that regulates UNC-40 asymmetric localization.

370

371 Robust clustering of UNC-40 is not a requirement for directed movement in response to
372 UNC-6. Indeed, even though there is a ventral directional bias for outgrowth towards the
373 UNC-6 source in *unc-53(n152);sax-3(ky200)* mutants, robust UNC-40::GFP asymmetric
374 localization is not observed (TANG AND WADSWORTH 2014). The ventral bias in the *unc-*
375 *53(n152);sax-3(ky200)* mutants is a response to UNC-6 since there is no ventral bias in *unc-*
376 *53(n152);sax-3(ky200);unc-6(ev400)* mutants. Similarly, in *sax-3(ky200)* and *unc-*
377 *5(e53);egl-20(n585)* mutants there is a ventral directional bias (Figure 4) but not robust
378 asymmetric UNC-40::GFP localization (Figure 6). The ventral directional bias in these
379 animals requires UNC-40 since in *unc-40(e1430),sax-3(ky200)* and *unc-40(e1430);egl-*
380 *20(n585)* mutants the ventral bias is compromised (Figure 4). Our interpretation is that
381 robust asymmetric UNC-40::GFP localization is a manifestation of the process that directs
382 the outgrowth in one direction rather than a prerequisite for directed outgrowth. In the *unc-*
383 *53(n152);sax-3(ky200), sax-3(ky200)*, and *unc-5(e53);egl-20(n585)* mutants the direction of

bioRxiv preprint doi: https://doi.org/10.1101/083436; this version posted October 25, 2016. The copyright holder for this preprint (which was not certified by peer review) is the author/funder, who has granted bioRxiv a license to display the preprint in perpetuity. It is made available under aCC-BY-NC-ND 4.0 International license.

outgrowth fluctuates enough so that strong clustering is not observed, but over time the bias creates ventral outgrowth.

We note that the HSN cell body can be misplaced posteriorly in *egl-20* mutants (WHANGBO AND KENYON 1999). This is a concern since the posterior environment might have different effects on extension and UNC-40::GFP asymmetric localization. However it was previously reported that the pattern of axon outgrowth extension is independent of the cell body position (KULKARNI *et al.* 2013). Moreover, the cell body is mispositioned in both *egl-20(n585)* and *unc-5(e53);egl-20(n585)* mutants but robust UNC-40::GFP asymmetric localization is only observed in *egl-20(n585)* mutants, suggesting that the lack of asymmetric localization in the *unc-5(e53);egl-20(n585)* mutants is due to *unc-5(e53)* rather than the position of the cell body.

MADD-2 is a cytoplasmic protein of the tripartite motif (TRIM) family that potentiates UNC-40 activity in response to UNC-6 (ALEXANDER *et al.* 2009; ALEXANDER *et al.* 2010; HAO *et al.* 2010; MORIKAWA *et al.* 2011; SONG *et al.* 2011; WANG *et al.* 2014). MADD-2::GFP and F-actin colocalize with UNC-40::GFP clusters in the anchor cell (WANG *et al.* 2014). It's been reported that in *madd-2* mutants UNC-40 localizes normally in neurons (HAO *et al.* 2010; SONG *et al.* 2011). Although its also been reported that UNC-40 will abnormally localize to the anterior and posterior surfaces of HSN (KULKARNI *et al.* 2013). UNC-40 localization in *madd-2* mutants was also reported to be defective in the anchor cell (WANG *et al.* 2014). There could be various reasons for the discrepancy, including different criteria for localization, different cell types, and the different alleles of *madd-2* that were used. In an investigation for localization in HSN, the *madd-2(ky592)* allele was used. The *madd-2(ky592)* allele is a strong loss-of-function allele. The *madd-2(tr103)* allele has also been

bioRxiv preprint doi: https://doi.org/10.1101/083436; this version posted October 25, 2016. The copyright holder for this preprint (which was not certified by peer review) is the author/funder, who has granted bioRxiv a license to display the preprint in perpetuity. It is made available under aCC-BY-NC-ND 4.0 International license.

409 used to show genetic interactions with *unc-40* and evidence indicates that this allele acts as
410 a genetic null (ALEXANDER *et al.* 2010). We therefore decided to test the *madd-2(tr103)*
411 allele in our UNC-40 localization assay. We find that this allele gives an even stronger
412 phenotype, *i.e.* robust UNC-40 asymmetric localization is not observed and the localization
413 is more uniform (Figure 6). This phenotype is similar to what is observe with *unc-6* and
414 *sax-3* mutants (KULKARNI *et al.* 2013; TANG AND WADSWORTH 2014).

415

416 **Discussion**

417 In this paper we show that UNC-5 regulates the number and length of neuronal processes
418 that a neuron can develop. We observe that *unc-5* loss-of-function mutations inhibit the
419 development of multiple neurites during early outgrowth from HSN. They also suppress the
420 development of extra HSN processes that are induced by a *mig-15* mutation or by
421 expression of the N-terminal fragment of UNC-6. We also observe that *unc-5* mutations
422 suppress the anterior overextension of the PLM axon that occurs in the *mig-15* mutant.
423 Finally, in combination with the *mig-15* mutation, *unc-5* loss-of-function mutations affect the
424 branching and extension of ALM and AVM axons at the nerve ring. In each of these cases,
425 the pattern of outgrowth is altered by loss of UNC-5 function. We further show that UNC-5
426 acts together with UNC-6, EGL-20, SAX-3, UNC-53, MIG-15, and MADD-2 to regulate UNC-
427 40 asymmetric localization at a surface of HSN. Here we discuss a model to explain how
428 UNC-5 could control these patterns of outgrowth by regulating UNC-40 asymmetric
429 localization.

430

431 **A model for the role UNC-5 plays in patterning neuronal outgrowth.**

bioRxiv preprint doi: https://doi.org/10.1101/083436; this version posted October 25, 2016. The copyright holder for this preprint (which was not certified by peer review) is the author/funder, who has granted bioRxiv a license to display the preprint in perpetuity. It is made available under aCC-BY-NC-ND 4.0 International license.

We have postulated that UNC-40 polarization is self-organizing and that the surface to which UNC-40 localizes and mediates outgrowth is stochastically determined (XU *et al.* 2009; KULKARNI *et al.* 2013). Genetic evidence indicates that UNC-40 conformational changes induced by UNC-6 ligation trigger multiple signals to coordinate the polarization and orientation processes (XU *et al.* 2009).

Because the surface to which UNC-40 localizes is stochastically determined, for each surface there is a probability that UNC-40-mediated outgrowth will take place there (Figure 7A). At any instance of time, extracellular cues govern this probability (KULKARNI *et al.* 2013; TANG AND WADSWORTH 2014; YANG *et al.* 2014). The machinery of UNC-40-mediated outgrowth creates forces that act on the membrane to cause extension and these forces act across the entire surface of the plasma membrane. Outgrowth extension can be envisioned as a serious of steps, and at each step the extracellular cues control the probability associated with movement in a particular direction. Therefore, the cues control the degree to which the direction of movement fluctuates over time. Such movement can be mathematically described as a random walk, *i.e*. a succession of randomly directed steps (Figure 3A). In contrast to straight-line or ballistic movement, random walk movement is diffusive and a property of diffusive motion is that the mean square displacement grows proportionate to the time traveled (Figure 5A). Consequently, the more the direction of movement fluctuates, the shorter the distance of travel in a given amount of time (Figure 7B). In the neuron, this diffusive motion occurs at the micro-scale at the membrane. An increase in diffusive motion at this scale might be observed at the macro-scale as a decrease in the relative rate of outgrowth. The patterns of outgrowth we observe are the product of all the probabilities for outgrowth that the extracellular cues determine at each instance of time.

bioRxiv preprint doi: https://doi.org/10.1101/083436; this version posted October 25, 2016. The copyright holder for this preprint (which was not certified by peer review) is the author/funder, who has granted bioRxiv a license to display the preprint in perpetuity. It is made available under aCC-BY-NC-ND 4.0 International license.

The combined effect of the extracellular cues sets a bias that determines the direction of outgrowth over time. Any variation from this state causes a higher probability of outgrowth in other directions. However, this does not necessarily cause movement in a new direction over time, but rather may only increase the back and forth fluctuation that occurs perpendicular to the direction of outgrowth. As illustrated in Figure 7B, this fluctuation reduces the extent of outgrowth over time without changing the overall direction of outgrowth. Because extracellular cues are not uniformly distributed in the extracellular environment, we postulate that the degree to which the direction of movement fluctuates can vary across the surface of the neuron. We propose that this variation can cause different regions of the neuron's membrane to move in the same direction but at different rates.

It is worth noting that our model does not directly address the molecular mechanisms through which the genes function. Rather, the use of random walks is a statistical approach to understand how a gene influences the collective impact of all the underlying molecular mechanisms that drive outgrowth. It can be envisioned that the movement of an extension occurs through innumerable forces acting at the molecular level. The effect that each molecular event has on movement is not easily observe or measured. In fact, it may be that patterns of outgrowth can't be fully understood by only knowing the molecular mechanisms of outgrowth. Instead, the effects that molecular events collectively have on movement must be understood through a statistical model.

bioRxiv preprint doi: https://doi.org/10.1101/083436; this version posted October 25, 2016. The copyright holder for this preprint (which was not certified by peer review) is the author/funder, who has granted bioRxiv a license to display the preprint in perpetuity. It is made available under aCC-BY-NC-ND 4.0 International license.

DCC (UNC-40) signaling occurs through different signaling complexes. One of these complexes involves DCC (UNC-40), UNC5 (UNC-5), and netrin-1 (UNC-6) (HONG *et al.* 1999; GEISBRECHT *et al.* 2003; KRUGER *et al.* 2004; FINCI *et al.* 2014). Our HSN results show that loss of UNC-5 function decreases the probability of UNC-40-mediated outgrowth towards the UNC-6 source and increases the probability of UNC-40-mediated outgrowth in other directions (Table 1and Figure 6). This promotes diffusive movement and, therefore, reduces the distance the membrane can travel in a given time (Figure 7A and 7B). We propose that UNC-5 is required for ventral extensions at the L1 stage and for the ventral migration of the cell body because it allows for a rate of outgrowth that is necessary for outward extensions to develop during this period of time (Figure 8A). Because movement is altered, the overall morphology of the HSN extension is abnormal, although the axon still develops and reaches the ventral nerve cord (Figure 1A).

The PLM neuron overextends in the *mig-15(rh148)* mutant and this overextension is suppressed by loss of UNC-40 or UNC-5 function (Figure 2D and 2E). In wildtype and in the *mig-15(rh148)* mutant, extracellular cues direct PLM outgrowth in the anterior direction. However, the normal extension of the PLM axon does not require UNC-40 or UNC-5 (HEDGECOCK *et al.* 1990). This suggests that the *mig-15(rh148)* mutation promotes UNC-40 and UNC-5 outgrowth activity and that in the *mig-15(rh148)* mutant UNC-40-mediated outgrowth activity is anteriorly directed. Similar to what is proposed for HSN, the loss of UNC-5 activity decreases the probability of UNC-40-mediated outgrowth in the anterior direction and increases the probability of UNC-40-mediated outgrowth in other directions. This promotes diffusive movement and reduces the distance outgrowth can travel in a given time (Figure 8A). The site of PLM axon termination may be set by the combined effect of all the extracellular cues at a particular location in the animal. Additional UNC-40 activity

bioRxiv preprint doi: https://doi.org/10.1101/083436; this version posted October 25, 2016. The copyright holder for this preprint (which was not certified by peer review) is the author/funder, who has granted bioRxiv a license to display the preprint in perpetuity. It is made available under aCC-BY-NC-ND 4.0 International license.

triggered by the *mig-15(rh148)* mutation may be enough to negate this effect, whereas the additional loss of UNC-5 activity nullifies the UNC-40 effect because it disperses the UNC-40-mediated outgrowth activity in other directions. That is, the probability of outgrowth in each direction could be set to the wild-type state by redistributing the direction of UNC-40 outgrowth activity.

The AVM axon branches to extend one process into the nerve ring and another anterior (Figure 2A). Our results indicate that extension into the nerve ring is dependent on UNC-40 activity and that loss of UNC-5 activity in the *mig-15(rh148)* mutant prevents extension into the nerve ring (Figure 2A and 2B). Similar to what we propose for HSN and PLM, we suggest that the *mig-15(rh148)* mutation causes addition UNC-40 outgrowth activity. In the *mig-15(rh148); unc-5(e53)* mutant the probability of UNC-40-mediated outgrowth in different directions increases and causes diffusive movement in every direction, inhibiting the rate of growth both into the nerve ring and anteriorly (Figure 8A). The *mig-15(rh148)* and the *unc-40(e1430)* mutations each has slight effects on the anterior extension but in combination have a stronger phenotype, suggesting that each plays an independent role in anterior extension (Figure 2C).

Our results show that UNC-5 can regulate the number of HSN processes that extend towards the UNC-6 source. To explain this, we suggest that UNC-40 (DCC), UNC-5 (UNC5), and UNC-6 (netrin) are part of an activator-inhibitor system (GIERER AND MEINHARDT 1972; MEINHARDT AND GIERER 2000). In an activator-inhibitor system two substance act on each other. The activator stimulates its own production as well as produces an inhibitor that can repress the production of the activator. The inhibitor is able to diffuse more rapidly than the activator, which causes patterns of varying concentrations of activator and inhibitor.

bioRxiv preprint doi: https://doi.org/10.1101/083436; this version posted October 25, 2016. The copyright holder for this preprint (which was not certified by peer review) is the author/funder, who has granted bioRxiv a license to display the preprint in perpetuity. It is made available under aCC-BY-NC-ND 4.0 International license.

We favor a model in which UNC-40 and UNC-5 are two substances that interact with each other (Figure 8B). This is consistent with evidence indicating that Netrin-1 binds simultaneously to two DCC (UNC-40) molecules or an UNC5/DCC complex (FINCI *et al.* 2014). In our model, UNC-5 signaling acts as an activator and UNC-40 signaling acts as an inhibitor. The activator and inhibitor activities "diffuse" at different rates because of the recruitment of UNC-40 and UNC-5 to the plasma membrane occurs at different rates. This idea is consistent with imaging experiments of cells in culture which suggest that netrin-1 (UNC-6) regulates the distribution of DCC (UNC-40) and UNC5B (UNC-5) at the plasma membrane (GOPAL *et al.* 2016). In these studies, netrin-1 (UNC-6) was shown to stimulate translocation of DCC (UNC-40) and UNC5B (UNC-5) receptors from intracellular vesicles to the plasma membrane and, further, the transported receptors were shown to localize at the plasma membrane (GOPAL *et al.* 2016).

We propose that signaling by UNC-6-ligated UNC-40 causes outgrowth activity and stimulates translocation of UNC-40 to the site (Figure 8B, step 1). If the outgrowth reaches a critical level of UNC-6 (Figure 8B, step 2), changes to the UNC-6/UNC-40/UNC-5 receptor complexes increases UNC-5 signaling (the activator). UNC-5 signaling inhibits UNC-40 translocation to the site and increases the relative levels of UNC-5 (short-range autocatalytic). Locally, UNC-40-mediated outgrowth activity becomes more dispersed, resulting in a slower rate of outgrowth. As UNC-40 translocation to the leading edge is inhibited, the level of UNC-40 at flanking surfaces increases (Figure 8B, step 3). These UNC-40 levels inhibits UNC-5 signaling (long-range inhibition) and prevents the dispersion of UNC-40-mediated outgrowth activity, resulting in a faster rate of outgrowth at the flanking surfaces.

bioRxiv preprint doi: https://doi.org/10.1101/083436; this version posted October 25, 2016. The copyright holder for this preprint (which was not certified by peer review) is the author/funder, who has granted bioRxiv a license to display the preprint in perpetuity. It is made available under aCC-BY-NC-ND 4.0 International license.

In this type of model, the reaction and diffusion rates of the substances influence the pattern that emerges. The *mig-15(rh148)* mutation and the expression of UNC-6ΔC could alter the rate by which components of the UNC-6/UNC-40/UNC-5 receptor complexes interact or alter the rate of translocation of the components to the membrane, or both. In fact, cell culture experiments suggest Netrin VI-V (UNC-6ΔC) induces DCC and UNC5B colocalization, but not DCC recruitment (GOPAL *et al.* 2016). Moreover, mutations that suppress ectopic branching induced by UNC-6ΔC expression affect members of second messenger systems which could influence the rates of UNC-40 and UNC-5 interactions and trafficking (WANG AND WADSWORTH 2002).

Genetic pathways for self-organizing UNC-40 asymmetric localization

We suggest genetic pathways for the functional order of action regulating the self-organization of UNC-40 polarization. These pathways are based on whether or not in different mutants UNC-40::GFP is observed to localize to any side of the HSN neuron (Figure 6). A summary of the results is presented (Figure 9A). We observe that UNC-6 is required for robust asymmetric UNC-40 localization; in the absence of UNC-6 function UNC-40 remains uniformly distributed along the surface of the plasma membrane. The loss of both UNC-53 and UNC-5 function also results in a uniform distribution, however loss of either one alone does not. This suggests that UNC-53 and UNC-5 pathways act redundantly downstream of UNC-6 (Figure 9B). Moreover, we observe there is robust asymmetric UNC-40 localization when there is a loss of UNC-6 activity in addition to the loss of UNC-53 and UNC-5. This suggests a third pathway that is suppressed by UNC-6 when UNC-53 and UNC-5 activity are missing. Loss of both UNC-5 and UNC-6 does not allow

bioRxiv preprint doi: https://doi.org/10.1101/083436; this version posted October 25, 2016. The copyright holder for this preprint (which was not certified by peer review) is the author/funder, who has granted bioRxiv a license to display the preprint in perpetuity. It is made available under aCC-BY-NC-ND 4.0 International license.

579 UNC-40 localization, whereas loss of both UNC-53 and UNC-6 does, therefore UNC-53,
580 rather than UNC-5, acts with UNC-6 to suppress the third pathway.

581

582 UNC-40 becomes localized when EGL-20 activity is lost. As well, UNC-40 becomes
583 localized when both EGL-20 and UNC-53 activities are lost. This is consistent with UNC-6
584 promoting UNC-40 localization via the UNC-5 pathway. Loss of EGL-20 and UNC-5
585 prevents UNC-40 localization. In these animals, the UNC-5 pathway is absent and UNC-6
586 is present to blocks the third pathway, therefore the UNC-53 pathway that leads to UNC-40
587 localization must require EGL-20, as well as UNC-6.

588

589 Loss of UNC-6 activity or loss of both UNC-6 and EGL-20 activity prevents localization,
590 whereas loss of only EGL-20 does not. To explain this, we propose that when UNC-6 is
591 lost, the third pathway, which would otherwise be activated by the loss of UNC-6, remains
592 suppressed because EGL-20 activity promotes suppression via UNC-53 activity. This
593 suppression also explains why loss of UNC-6 and UNC-5 activity does not cause
594 localization.

595

596 Importantly, this genetic analysis indicates that netrin (UNC-6) and wnt (EGL-20) signaling
597 are integrated to regulate self-organizing UNC-40 asymmetric localization. An implication of
598 this result is that the extracellular concentrations of UNC-6 and EGL-20 could control the
599 activation or inhibition of UNC-40-mediated outgrowth.

600

601

bioRxiv preprint doi: https://doi.org/10.1101/083436; this version posted October 25, 2016. The copyright holder for this preprint (which was not certified by peer review) is the author/funder, who has granted bioRxiv a license to display the preprint in perpetuity. It is made available under aCC-BY-NC-ND 4.0 International license.

602 # Table

603

604

Table 1. Direction of Axon Formation from the HSN Cell Body

	direction of axon protrusion						
	dorsal	ventral	anterior	posterior	multipolar		
	%	%	%	%	%	*n*	reference
wild-type	0	96±2	3±2	0	1±1	221	(KULKARNI *et al.* 2013)
unc-6(ev400)	2±2	3±2	81±2	8±2	6±1	218	(KULKARNI *et al.* 2013)
unc-40(e1430)	2±1	6±2	67±2	19±1	6±1	183	(KULKARNI *et al.* 2013)
unc-5(e53)	0	75±3	19±2	1±1	5±1	245	(YANG *et al.* 2014)
unc-53(n152)	0	67±3	22±2	5±1	6±1	238	(KULKARNI *et al.* 2013)
sax-3(ky123)	2±1	31±1	21±1	37±2	9±2	232	(TANG AND WADSWORTH 2014)
*sax-3(ky200)**	2±1	32±1	19±2	42±3	5±2	198	(TANG AND WADSWORTH 2014)
unc-5(e53);sax-3(ky200)	2±1	40±3	24±2	28±2	6±1	120	
unc-5(e53);unc-6(ev400)	4±2	5±3	59±4	22±4	9±1	201	
unc-5(e53);egl-20(n585)	3±1	28±4	22±4	35±5	11±2	114	
unc-53(n152);unc-5(e53)	0	19±1	62±2	17±1	3±1	224	(KULKARNI *et al.* 2013)
unc-53(n152);unc-6(ev400)	24±2	0	19±2	22±2	34±3	144	(KULKARNI *et al.* 2013)
unc-53(n152);sax-3(ky123)	1±1	47±3	24±2	23±5	6±3	207	(TANG AND WADSWORTH 2014)
unc-40(e1430);unc-5(e53)	5±1	6±1	55±2	19±2	14±1	196	(KULKARNI *et al.* 2013)
*unc-40(e1430);sax-3(ky200)**	14±3	2±1	40±2	35±3	9±4	191	(TANG AND WADSWORTH 2014)
sax-3(ky200); unc-6(ev400)*	8±1	8±2	49±3	20±5	14±2	211	(TANG AND WADSWORTH 2014)
unc-53(n152);unc-5(e53);unc-6(ev400)	23±2	0	34±2	15±2	28±2	148	(KULKARNI *et al.* 2013)
unc-53(n152);sax-3(ky200);unc-6(ev400)*	11±2	2±1	33±4	30±3	25±5	189	
egl-20(n585)	0	64±2	21±2	7±1	8±1	304	(TANG AND WADSWORTH 2014)
egl-20(n585); unc-6(ev400)	18±2	0	43±2	15±2	24±2	205	(TANG AND WADSWORTH 2014)
unc-40(e1430); egl-20(n585)	6±2	17±2	45±5	15±2	16±2	173	(TANG AND WADSWORTH 2014)
egl-20(n585);sax-3(ky123)	1±1	12±2	39±2	39±1	8±3	177	(TANG AND WADSWORTH 2014)
madd-2(tr103)	0	19±2	55±5	17±4	8±2	179	
madd-2(ky592)	0	52±2	43±2	5±1	0	95	
unc-5(e53);madd-2(tr103)	3±1	15±2	52±4	17±4	13±1	197	
madd-2(tr103);sax-3(ky123)	2	24±3	19±4	47±1	7±2	171	
unc-53(n152);madd-2(tr103)	1±1	15±2	43±2	17±1	24±4	148	
mig-15(rh326)	2±1	15±1	24±3	11±3	48±8	131	(YANG *et al.* 2014)

Numbers represent percentage value ± SEM.

*Animals grown at the *sax-3(ky200)* restrictive temperature (25°C).

605

bioRxiv preprint doi: https://doi.org/10.1101/083436; this version posted October 25, 2016. The copyright holder for this preprint (which was not certified by peer review) is the author/funder, who has granted bioRxiv a license to display the preprint in perpetuity. It is made available under aCC-BY-NC-ND 4.0 International license.

606 **References**

607 Adler, C. E., R. D. Fetter and C. I. Bargmann, 2006 UNC-6/Netrin induces neuronal
608 asymmetry and defines the site of axon formation. Nat Neurosci 9**:** 511-518.

609 Alexander, M., K. K. Chan, A. B. Byrne, G. Selman, T. Lee *et al.*, 2009 An UNC-40 pathway
610 directs postsynaptic membrane extension in Caenorhabditis elegans. Development 136**:**
611 911-922.

612 Alexander, M., G. Selman, A. Seetharaman, K. K. Chan, S. A. D'Souza *et al.*, 2010 MADD-
613 2, a homolog of the Opitz syndrome protein MID1, regulates guidance to the midline through
614 UNC-40 in Caenorhabditis elegans. Developmental Cell 18**:** 961-972.

615 Asakura, T., K. Ogura and Y. Goshima, 2007 UNC-6 expression by the vulval precursor
616 cells of Caenorhabditis elegans is required for the complex axon guidance of the HSN
617 neurons. Dev Biol 304**:** 800-810.

618 Bernadskaya, Y. Y., A. Wallace, J. Nguyen, W. A. Mohler and M. C. Soto, 2012 UNC-
619 40/DCC, SAX-3/Robo, and VAB-1/Eph polarize F-actin during embryonic morphogenesis by
620 regulating the WAVE/SCAR actin nucleation complex. PLoS Genet 8**:** e1002863.

621 Bhat, J. M., and H. Hutter, 2016 Pioneer Axon Navigation Is Controlled by AEX-3, a
622 Guanine Nucleotide Exchange Factor for RAB-3 in Caenorhabditis elegans. Genetics.

623 Chan, S. S., H. Zheng, M. W. Su, R. Wilk, M. T. Killeen *et al.*, 1996 UNC-40, a C. elegans
624 homolog of DCC (Deleted in Colorectal Cancer), is required in motile cells responding to
625 UNC-6 netrin cues. Cell 87**:** 187-195.

626 Chang, C., C. E. Adler, M. Krause, S. G. Clark, F. B. Gertler *et al.*, 2006 MIG-
627 10/Lamellipodin and AGE-1/PI3K Promote Axon Guidance and Outgrowth in Response to
628 Slit and Netrin. Curr Biol 16**:** 854-862.

629 Chapman, J. O., H. Li and E. A. Lundquist, 2008 The MIG-15 NIK kinase acts cell-
630 autonomously in neuroblast polarization and migration in C. elegans. Dev Biol 324**:** 245-
631 257.

632 Finci, L. I., N. Krüger, X. Sun, J. Zhang, M. Chegkazi *et al.*, 2014 The crystal structure of
633 netrin-1 in complex with DCC reveals the bifunctionality of netrin-1 as a guidance cue.
634 Neuron 83**:** 839-849.

635 Geisbrecht, B. V., K. A. Dowd, R. W. Barfield, P. A. Longo and D. J. Leahy, 2003 Netrin
636 binds discrete subdomains of DCC and UNC5 and mediates interactions between DCC and
637 heparin. J Biol Chem 278**:** 32561-32568.

bioRxiv preprint doi: https://doi.org/10.1101/083436; this version posted October 25, 2016. The copyright holder for this preprint (which was not certified by peer review) is the author/funder, who has granted bioRxiv a license to display the preprint in perpetuity. It is made available under aCC-BY-NC-ND 4.0 International license.

638 Gierer, A., and H. Meinhardt, 1972 A theory of biological pattern formation. Kybernetik 12**:**
639 30-39.

640 Gopal, A. A., B. Rappaz, V. Rouger, I. B. Martyn, P. D. Dahlberg *et al.*, 2016 Netrin-1-
641 Regulated Distribution of UNC5B and DCC in Live Cells Revealed by TICCS. Biophys J
642 110**:** 623-634.

643 Hao, J. C., C. E. Adler, L. Mebane, F. B. Gertler, C. I. Bargmann *et al.*, 2010 The tripartite
644 motif protein MADD-2 functions with the receptor UNC-40 (DCC) in Netrin-mediated axon
645 attraction and branching. Dev Cell 18**:** 950-960.

646 Hedgecock, E. M., J. G. Culotti and D. H. Hall, 1990 The unc-5, unc-6, and unc-40 genes
647 guide circumferential migrations of pioneer axons and mesodermal cells on the epidermis in
648 C. elegans. Neuron 4**:** 61-85.

649 Hong, K., L. Hinck, M. Nishiyama, M. M. Poo, M. Tessier-Lavigne *et al.*, 1999 A ligand-gated
650 association between cytoplasmic domains of UNC5 and DCC family receptors converts
651 netrin-induced growth cone attraction to repulsion. Cell 97**:** 927-941.

652 Keleman, K., and B. J. Dickson, 2001 Short- and long-range repulsion by the Drosophila
653 Unc5 netrin receptor. Neuron 32**:** 605-617.

654 Killeen, M., J. Tong, A. Krizus, R. Steven, I. Scott *et al.*, 2002 UNC-5 function requires
655 phosphorylation of cytoplasmic tyrosine 482, but its UNC-40-independent functions also
656 require a region between the ZU-5 and death domains. Dev Biol 251**:** 348-366.

657 Kruger, R. P., J. Lee, W. Li and K. L. Guan, 2004 Mapping netrin receptor binding reveals
658 domains of Unc5 regulating its tyrosine phosphorylation. J Neurosci 24**:** 10826-10834.

659 Kulkarni, G., Z. Xu, A. M. Mohamed, H. Li, X. Tang *et al.*, 2013 Experimental evidence for
660 UNC-6 (netrin) axon guidance by stochastic fluctuations of intracellular UNC-40 (DCC)
661 outgrowth activity. Biol Open 2**:** 1300-1312.

662 Leung-Hagesteijn, C., A. M. Spence, B. D. Stern, Y. Zhou, M. W. Su *et al.*, 1992 UNC-5, a
663 transmembrane protein with immunoglobulin and thrombospondin type 1 domains, guides
664 cell and pioneer axon migrations in C. elegans. Cell 71**:** 289-299.

665 Levy-Strumpf, N., and J. G. Culotti, 2007 VAB-8, UNC-73 and MIG-2 regulate axon polarity
666 and cell migration functions of UNC-40 in C. elegans. Nat Neurosci 10**:** 161-168.

667 Levy-Strumpf, N., and J. G. Culotti, 2014 Netrins and Wnts function redundantly to regulate
668 antero-posterior and dorso-ventral guidance in C. elegans. PLoS Genet 10**:** e1004381.

bioRxiv preprint doi: https://doi.org/10.1101/083436; this version posted October 25, 2016. The copyright holder for this preprint (which was not certified by peer review) is the author/funder, who has granted bioRxiv a license to display the preprint in perpetuity. It is made available under aCC-BY-NC-ND 4.0 International license.

669 Levy-Strumpf, N., M. Krizus, H. Zheng, L. Brown and J. G. Culotti, 2015 The Wnt Frizzled
670 Receptor MOM-5 Regulates the UNC-5 Netrin Receptor through Small GTPase-Dependent
671 Signaling to Determine the Polarity of Migrating Cells. PLoS Genet 11: e1005446.

672 Li, H., G. Kulkarni and W. G. Wadsworth, 2008 RPM-1, a Caenorhabditis elegans protein
673 that functions in presynaptic differentiation, negatively regulates axon outgrowth by
674 controlling SAX-3/robo and UNC-5/UNC5 activity. J Neurosci 28: 3595-3603.

675 Lim, Y. S., S. Mallapur, G. Kao, X. C. Ren and W. G. Wadsworth, 1999 Netrin UNC-6 and
676 the regulation of branching and extension of motoneuron axons from the ventral nerve cord
677 of Caenorhabditis elegans. J Neurosci 19: 7048-7056.

678 Meinhardt, H., and A. Gierer, 2000 Pattern formation by local self-activation and lateral
679 inhibition. Bioessays 22: 753-760.

680 Merz, D. C., H. Zheng, M. T. Killeen, A. Krizus and J. G. Culotti, 2001 Multiple signaling
681 mechanisms of the unc-6/netrin receptors unc-5 and unc-40/dcc in vivo. Genetics 158:
682 1071-1080.

683 Moore, S. W., M. Tessier-Lavigne and T. E. Kennedy, 2007 Netrins and their receptors. Adv
684 Exp Med Biol 621: 17-31.

685 Morikawa, R. K., T. Kanamori, K. Yasunaga and K. Emoto, 2011 Different levels of the
686 Tripartite motif protein, Anomalies in sensory axon patterning (Asap), regulate distinct
687 axonal projections of Drosophila sensory neurons. Proc Natl Acad Sci U S A 108: 19389-
688 19394.

689 Norris, A. D., and E. A. Lundquist, 2011 UNC-6/netrin and its receptors UNC-5 and UNC-
690 40/DCC modulate growth cone protrusion in vivo in C. elegans. Development.

691 Pan, C. L., J. E. Howell, S. G. Clark, M. Hilliard, S. Cordes *et al.*, 2006 Multiple Wnts and
692 frizzled receptors regulate anteriorly directed cell and growth cone migrations in
693 Caenorhabditis elegans. Dev Cell 10: 367-377.

694 Poinat, P., A. De Arcangelis, S. Sookhareea, X. Zhu, E. M. Hedgecock *et al.*, 2002 A
695 conserved interaction between beta1 integrin/PAT-3 and Nck-interacting kinase/MIG-15 that
696 mediates commissural axon navigation in C. elegans. Curr Biol 12: 622-631.

697 Quinn, C. C., D. S. Pfeil, E. Chen, E. L. Stovall, M. V. Harden *et al.*, 2006 UNC-6/netrin and
698 SLT-1/slit guidance cues orient axon outgrowth mediated by MIG-10/RIAM/lamellipodin.
699 Curr Biol 16: 845-853.

bioRxiv preprint doi: https://doi.org/10.1101/083436; this version posted October 25, 2016. The copyright holder for this preprint (which was not certified by peer review) is the author/funder, who has granted bioRxiv a license to display the preprint in perpetuity. It is made available under aCC-BY-NC-ND 4.0 International license.

Shakir, M. A., J. S. Gill and E. A. Lundquist, 2006 Interactions of UNC-34 Enabled with Rac GTPases and the NIK kinase MIG-15 in Caenorhabditis elegans axon pathfinding and neuronal migration. Genetics 172**:** 893-913.

Song, S., Q. Ge, J. Wang, H. Chen, S. Tang *et al.*, 2011 TRIM-9 functions in the UNC-6/UNC-40 pathway to regulate ventral guidance. Journal of genetics and genomics = Yi chuan xue bao 38**:** 1-11.

Tang, X., and W. G. Wadsworth, 2014 SAX-3 (Robo) and UNC-40 (DCC) Regulate a Directional Bias for Axon Guidance in Response to Multiple Extracellular Cues. PLoS One 9**:** e110031.

Teulière, J., C. Gally, G. Garriga, M. Labouesse and E. Georges-Labouesse, 2011 MIG-15 and ERM-1 promote growth cone directional migration in parallel to UNC-116 and WVE-1. Development 138**:** 4475-4485.

Wadsworth, W. G., H. Bhatt and E. M. Hedgecock, 1996 Neuroglia and pioneer neurons express UNC-6 to provide global and local netrin cues for guiding migrations in C. elegans. Neuron 16**:** 35-46.

Wadsworth, W. G., and E. M. Hedgecock, 1996 Hierarchical guidance cues in the developing nervous system of C. elegans. Bioessays 18**:** 355-362.

Wang, Q., and W. G. Wadsworth, 2002 The C domain of netrin UNC-6 silences calcium/calmodulin-dependent protein kinase- and diacylglycerol-dependent axon branching in Caenorhabditis elegans. J Neurosci 22**:** 2274-2282.

Wang, Z., L. M. Linden, K. M. Naegeli, J. W. Ziel, Q. Chi *et al.*, 2014 UNC-6 (netrin) stabilizes oscillatory clustering of the UNC-40 (DCC) receptor to orient polarity. J Cell Biol 206**:** 619-633.

Watari-Goshima, N., K. Ogura, F. W. Wolf, Y. Goshima and G. Garriga, 2007 C. elegans VAB-8 and UNC-73 regulate the SAX-3 receptor to direct cell and growth-cone migrations. Nat Neurosci 10**:** 169-176.

Whangbo, J., and C. Kenyon, 1999 A Wnt signaling system that specifies two patterns of cell migration in C. elegans. Molecular cell 4**:** 851-858.

Xu, Z., H. Li and W. G. Wadsworth, 2009 The roles of multiple UNC-40 (DCC) receptor-mediated signals in determining neuronal asymmetry induced by the UNC-6 (netrin) ligand. Genetics 183**:** 941-949.

bioRxiv preprint doi: https://doi.org/10.1101/083436; this version posted October 25, 2016. The copyright holder for this preprint (which was not certified by peer review) is the author/funder, who has granted bioRxiv a license to display the preprint in perpetuity. It is made available under aCC-BY-NC-ND 4.0 International license.

731 Yang, Y., W. S. Lee, X. Tang and W. G. Wadsworth, 2014 Extracellular Matrix Regulates
732 UNC-6 (Netrin) Axon Guidance by Controlling the Direction of Intracellular UNC-40 (DCC)
733 Outgrowth Activity. PLoS One 9**:** e97258.

734

bioRxiv preprint doi: https://doi.org/10.1101/083436; this version posted October 25, 2016. The copyright holder for this preprint (which was not certified by peer review) is the author/funder, who has granted bioRxiv a license to display the preprint in perpetuity. It is made available under aCC-BY-NC-ND 4.0 International license.

Legends

Figure 1. UNC-5 regulates the patterning of outgrowth extensions from HSN. (**A**) Photomicrographs of HSN at the L1, L2, and adult stages in wild-type and *unc-5(e53)* mutants. In L1 and L2 animals neurite extensions (arrows) are often observed in wild-type animals but are more rare in *unc-5* mutants. The short ventral migration of the cell body that occurs in wild-type animal sometimes fails in *unc-5* mutants, leaving the cell body farther from the PLM axon (arrowhead) with a single longer ventral extension. The position of the cell body remains dorsal. Scale bar: 10 μm. (**B**) The percentage of HSN neuron with 0, 1, or more than 1 neurite extension at the L1 stage. In *unc-5* mutants nearly half of the neurons do not extend a process. Error bars indicated the standard error mean; n values are indicated above each column. Significant differences (two-tailed t-test), *P<0.001. (**C**) The percentage of HSN neurons with a single long extension at the L2 stage. Several *unc-5* alleles were tested as described in the text. In mutants with loss-of-function there is more often a single extension from the cell body and the cell body is dorsally mispositioned. (**D**) Photomicrographs of HSN at the early L4, late L4, and adult stages in wild-type and in animals expressing UNC-6ΔC. The expression of UNC-6ΔC induces multiple processes, most often two major extensions, that are guided ventrally. (**E**) The percentage of HSN neurons with a cell body mispositioned dorsally at the L2 stage. In loss-of-function mutants the cell body often fails to undertake a short ventral migration during the L2 stage. The migration is not delayed, but rather it remains dorsal. (**F**) The percentage of HSN neurons with multiple ventral extensions at the L4 stage. The additional processes induced by UNC-6ΔC can be suppressed by *unc-5* and *mig-10* mutations. Additional processes induced by *mig-15(rh148)* can also be suppressed by the *unc-5* mutation. (**G**) Photomicrographs of HSN at adult stages in a *mig-15* mutant. Similar to UNC-6ΔC expression, *mig-15* mutations can also cause additional processes that are guided ventrally (YANG *et al.* 2014).

bioRxiv preprint doi: https://doi.org/10.1101/083436; this version posted October 25, 2016. The copyright holder for this preprint (which was not certified by peer review) is the author/funder, who has granted bioRxiv a license to display the preprint in perpetuity. It is made available under aCC-BY-NC-ND 4.0 International license.

760

bioRxiv preprint doi: https://doi.org/10.1101/083436; this version posted October 25, 2016. The copyright holder for this preprint (which was not certified by peer review) is the author/funder, who has granted bioRxiv a license to display the preprint in perpetuity. It is made available under aCC-BY-NC-ND 4.0 International license.

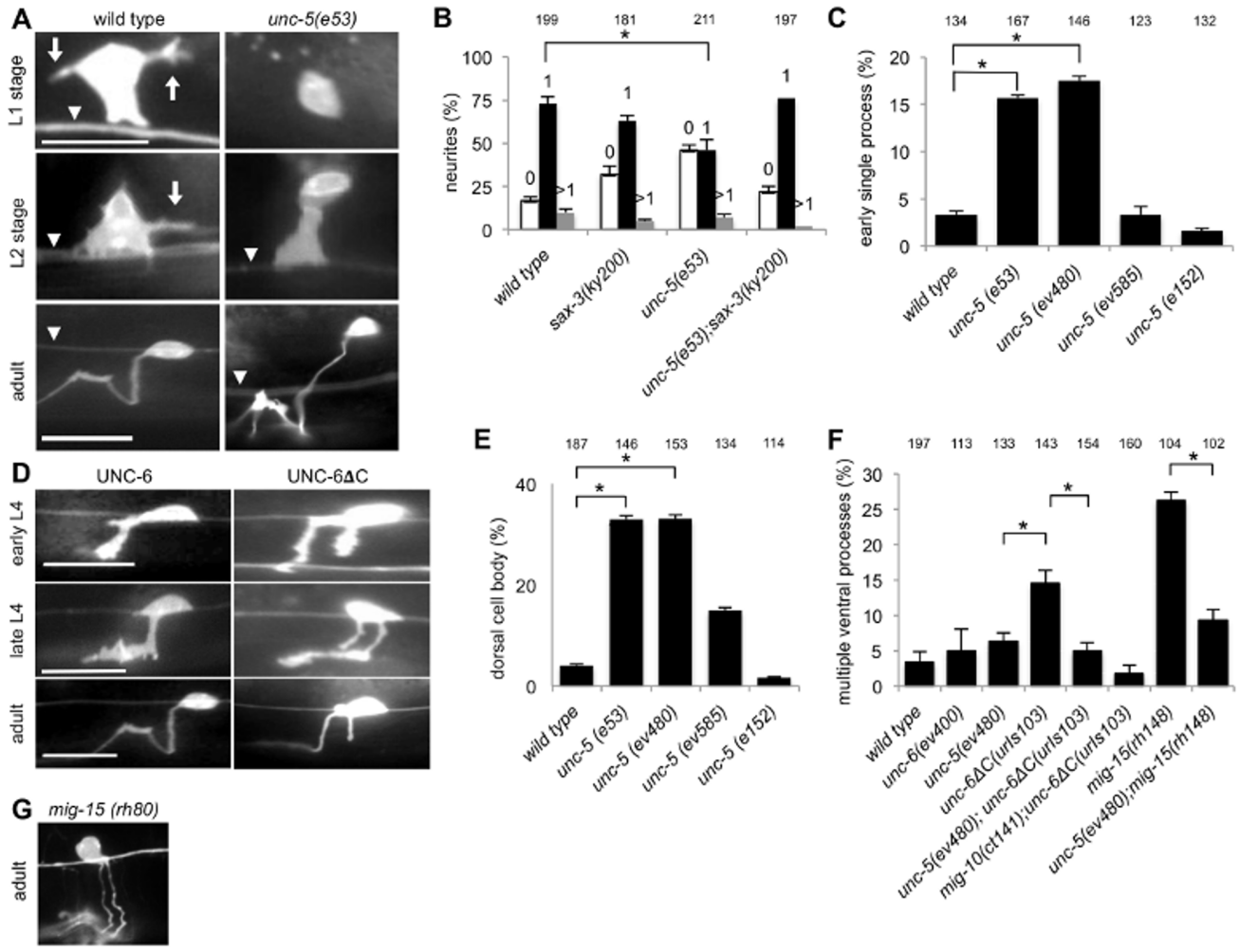

761

762

bioRxiv preprint doi: https://doi.org/10.1101/083436; this version posted October 25, 2016. The copyright holder for this preprint (which was not certified by peer review) is the author/funder, who has granted bioRxiv a license to display the preprint in perpetuity. It is made available under aCC-BY-NC-ND 4.0 International license.

Figure 2. UNC-5 regulates the patterning of extension from ALM, AVM, and PLM. (**A**) Photomicrographs of the ALM and AVM neurons at the L4 stage in wild-type animals and mutants showing different patterns of outgrowth extension. In wild type (top) a single axon travels anteriorly to the nerve ring (arrowheads). At the nerve ring the axon branches; one branch extends further anteriorly and the other extends into the nerve ring. In mutants, one or both axons may only extend anteriorly and will not extend into the nerve ring (second from top). Or one or both axons will only extend into the nerve ring and will not extend anteriorly (third from top). Or one or both axons will fail to extend into either the nerve ring or anteriorly (bottom). Scale bar: 20 μm. (**B**) The percentage of AVM neurons where the AVM neuron failed to extend into the nerve ring. The neuron often fails to extend in the *unc-40* and *mig-15;unc-5* mutants, whereas it does extend in the *mig-15, unc-5,* and *mig-15;unc-40* mutants. Error bars indicated the standard error mean; n values are indicated above each column. Significant differences (two-tailed t-test), *P<0.001. (**C**) The percentage of AVM neurons where the AVM neuron failed to extend anteriorly, past the nerve ring. The neuron often fails to extend anteriorly in the *mig-15;unc-5* mutants, whereas it does extend in the *mig-15, unc-5, unc-40,* and *unc-40;mig-15* mutants. There is a significant difference between the *unc-40* and *unc-40;mig-15* mutants. (**D**) Photomicrographs of the ALM, AVM, and PLM neurons at the L4 stage in wild-type animals and *mig-15* mutants. In wild type (top) a single PLM axon travels anteriorly from the posterior cell body (not shown). Near the vulva (arrow) the axon branches; one branch extends to the ventral nerve chord and another extends anteriorly. The anterior extension terminates before reaching the area of the ALM cell body. In *mig-15* mutants the PLM can extend anteriorly past the ALM cell body (bottom). (**E**) The percentage of PLM neurons where the PLM neuron extend anteriorly past the ALM cell body. The anterior extension often over-extends in *mig-15* mutants. Loss of *unc-5* or *unc-40* function can suppress this phenotype.

bioRxiv preprint doi: https://doi.org/10.1101/083436; this version posted October 25, 2016. The copyright holder for this preprint (which was not certified by peer review) is the author/funder, who has granted bioRxiv a license to display the preprint in perpetuity. It is made available under aCC-BY-NC-ND 4.0 International license.

788

bioRxiv preprint doi: https://doi.org/10.1101/083436; this version posted October 25, 2016. The copyright holder for this preprint (which was not certified by peer review) is the author/funder, who has granted bioRxiv a license to display the preprint in perpetuity. It is made available under aCC-BY-NC-ND 4.0 International license.

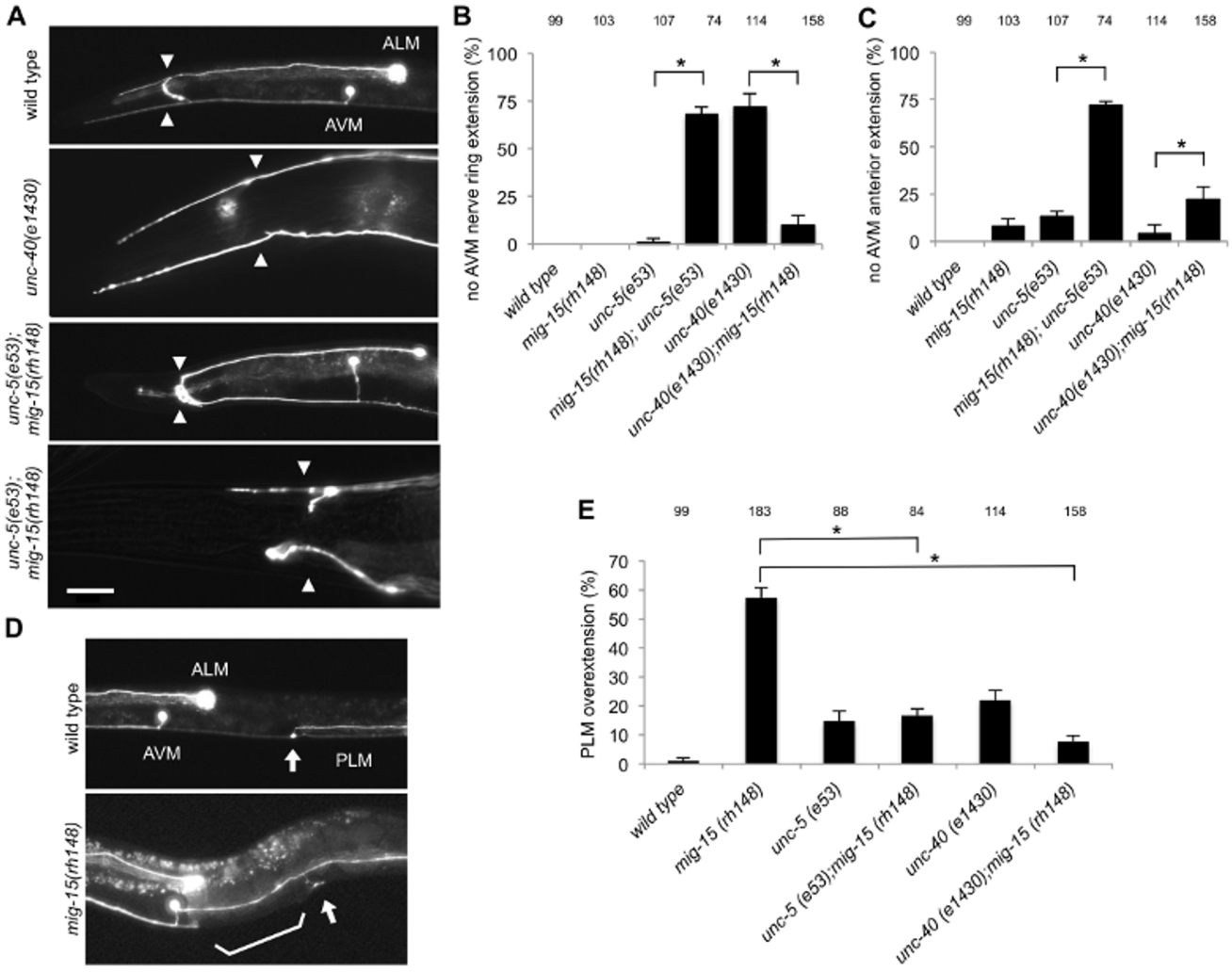

bioRxiv preprint doi: https://doi.org/10.1101/083436; this version posted October 25, 2016. The copyright holder for this preprint (which was not certified by peer review) is the author/funder, who has granted bioRxiv a license to display the preprint in perpetuity. It is made available under aCC-BY-NC-ND 4.0 International license.

Figure 3. Assay to measure the effects a mutation has on movement. (**A**) The direction of outgrowth extension from the HSN cell body can vary and whether the axon developed in the dorsal, anterior, posterior, or ventral direction in L4 stage animals is scored (left panel). This creates a probability distribution in which the direction (*X*) is a random variable (center panel). A simple random walk is generated by using the same probability distribution for a succession of steps with an equal time interval (right panel). (**B**) For wild type and two mutants, 50 simulated random walks of 500 steps were plotted from an origin (0,0). The results graphically indicate the directional bias for movement. For random walk movement created in mutant A (red, results from *unc-5(e53)*), the directional bias is shifted anteriorly (left) relative to wild type. The results also graphically show the displacement of movement. For random walk movement created in mutant B (blue, results from *egl-20(n585);sax-3(ky123)*), the average of the final position (displacement) from the origin is a much shorter distance than wild type. (**C**) Plots of the normal distribution of the final position along the x axis of the random walk tracks shown in B. The mean position for each is set at 0. The plots graphically illustrate how random walks constructed from the probability distribution for the direction of outgrowth extensions can reveal a diffusion process.

bioRxiv preprint doi: https://doi.org/10.1101/083436; this version posted October 25, 2016. The copyright holder for this preprint (which was not certified by peer review) is the author/funder, who has granted bioRxiv a license to display the preprint in perpetuity. It is made available under aCC-BY-NC-ND 4.0 International license.

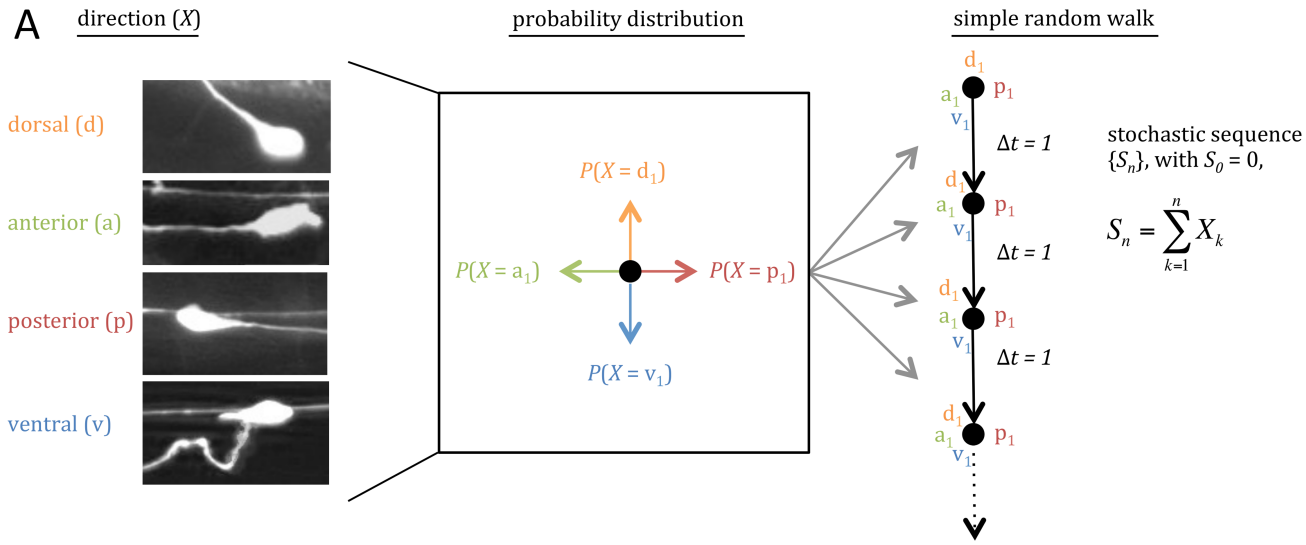

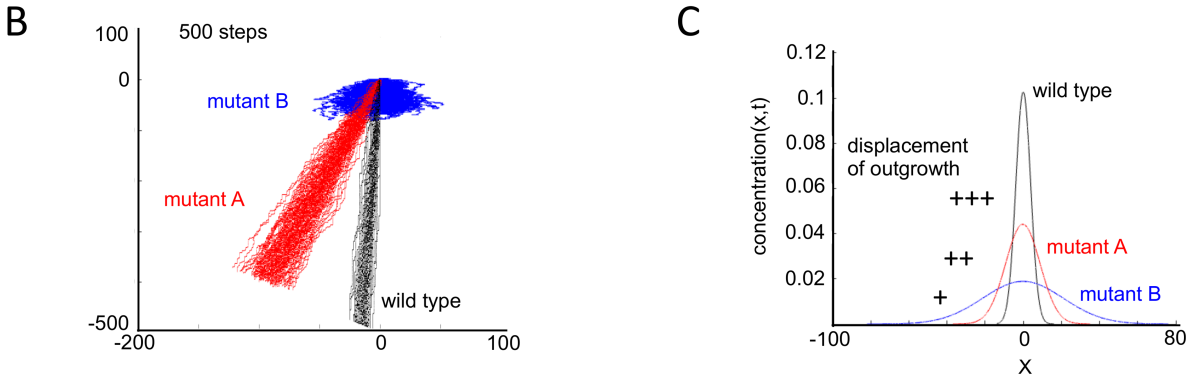

808

809

bioRxiv preprint doi: https://doi.org/10.1101/083436; this version posted October 25, 2016. The copyright holder for this preprint (which was not certified by peer review) is the author/funder, who has granted bioRxiv a license to display the preprint in perpetuity. It is made available under aCC-BY-NC-ND 4.0 International license.

Figure 4. Mutations have different effects on movement. Examples of random walk analyses using the direction of axon development from the HSN neuron in different mutants (Table 1). The graphs were created as described in the figure legend of Figure 1. For each panel, plots are shown for the normal distribution of the final position along the x axis for the random walk tracks plotted in the inserts. The inserts depict the random walk movement that would be produced by the probability distribution for the direction of outgrowth in the mutant. Plots derived from the same data are colored alike. Each panel depicts the analyses of four different mutants and wild type. Three different distribution patterns are observed: (1) the wild-type distribution, which has the distribution curve with the highest peak; (2) the *unc-5, egl-20, unc-53,* and *unc-6* (not shown) distribution, which is flatter than the wild-type curve; (3) the *madd-2, sax-3, mig-15,* and double combinations, which have the flattest distribution curve.

bioRxiv preprint doi: https://doi.org/10.1101/083436; this version posted October 25, 2016. The copyright holder for this preprint (which was not certified by peer review) is the author/funder, who has granted bioRxiv a license to display the preprint in perpetuity. It is made available under aCC-BY-NC-ND 4.0 International license.

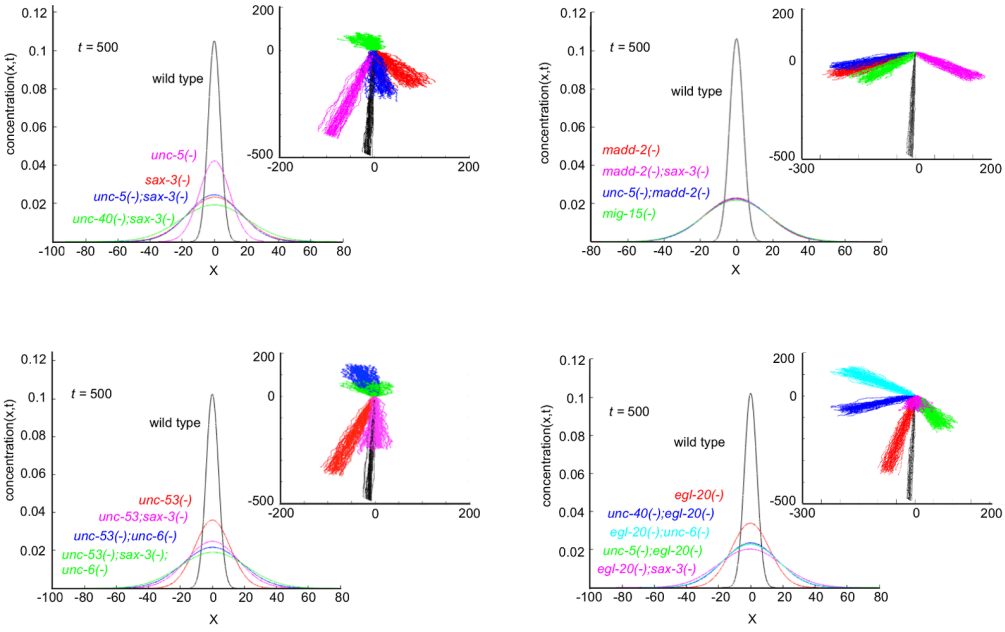

823

824

bioRxiv preprint doi: https://doi.org/10.1101/083436; this version posted October 25, 2016. The copyright holder for this preprint (which was not certified by peer review) is the author/funder, who has granted bioRxiv a license to display the preprint in perpetuity. It is made available under aCC-BY-NC-ND 4.0 International license.

825 **Figure 5. Mutations alter the spatial extent of movement.** (**A**) Plotted are the mean
826 squared displacement (MSD) curves as a function of time interval (d*t*). The values are in
827 arbitrary units, since the time scale was arbitrarily set at 1. The curves show the extent that
828 different mutations can alter the MSD relative to wild type and the MSD caused by an
829 unbiased random walk. For each time interval, mean and s.e.m. are plotted. (**B**) From the
830 slope of MSD curves a coefficient can be derived that gives the relative rate of diffusion.
831 Colored bars correspond to the like-colored curves given in panel A. The coefficients for
832 *unc-5, egl-20, unc-53,* and *unc-6* form a class that is distinct from that derived from wild type
833 and from the double mutants.
834

bioRxiv preprint doi: https://doi.org/10.1101/083436; this version posted October 25, 2016. The copyright holder for this preprint (which was not certified by peer review) is the author/funder, who has granted bioRxiv a license to display the preprint in perpetuity. It is made available under aCC-BY-NC-ND 4.0 International license.

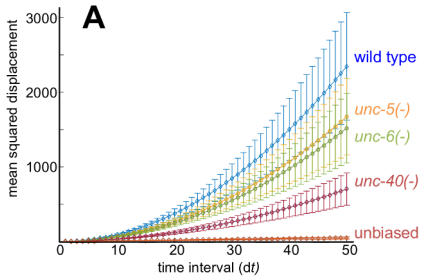

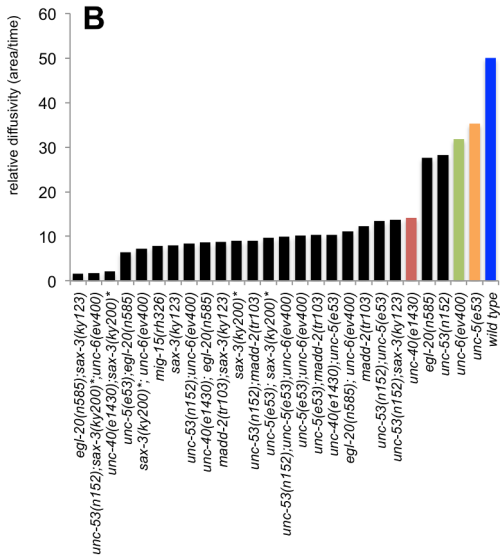

835

836

bioRxiv preprint doi: https://doi.org/10.1101/083436; this version posted October 25, 2016. The copyright holder for this preprint (which was not certified by peer review) is the author/funder, who has granted bioRxiv a license to display the preprint in perpetuity. It is made available under aCC-BY-NC-ND 4.0 International license.

837 **Figure 6. Mutations affect asymmetric intracellular UNC-40::GFP localization.** (**A**)
838 Graph indicating the dorsal-ventral localization of UNC-40::GFP in HSN. The graph shows
839 the average ratio of dorsal-to-ventral intensity from linescan intensity plots of the UNC-
840 40::GFP signal around the periphery of the HSN cell. UNC-40::GFP is ventrally localized in
841 wild-type, but the ratio is different in the mutants. Error bars represent standard error of
842 mean. Below is a graphic representation of the possible UNC-40 localization patterns when
843 the intensity ratio is ≥ 1 or is <1. (**B**) Graph indicating the anterior-posterior localization of
844 UNC-40::GFP. To determine orientation, line-scan intensity plots of the UNC-40::GFP
845 signal across the dorsal periphery of the HSN cell were taken, the dorsal surface was
846 geometrically divided into three equal segments, and the total intensity of each was
847 recorded. The percent intensity was calculated for each segment and ANOVA was used to
848 determine if there is a significant difference between the three segments (see Material and
849 Methods). Whereas in the *unc-5* and *egl-20* mutants there is a bias for anterior or posterior
850 localization, there is a uniform distribution in *unc-5;egl-20* double mutants. Uniform
851 distribution is also observed in strong loss-of-function *sax-3* and *madd-2* mutants. (*)
852 Animals grown at the *sax-3(ky200)* restrictive temperature (25°C). Below is a graphic
853 representation of the possible UNC-40 localization patterns.
854

bioRxiv preprint doi: https://doi.org/10.1101/083436; this version posted October 25, 2016. The copyright holder for this preprint (which was not certified by peer review) is the author/funder, who has granted bioRxiv a license to display the preprint in perpetuity. It is made available under aCC-BY-NC-ND 4.0 International license.

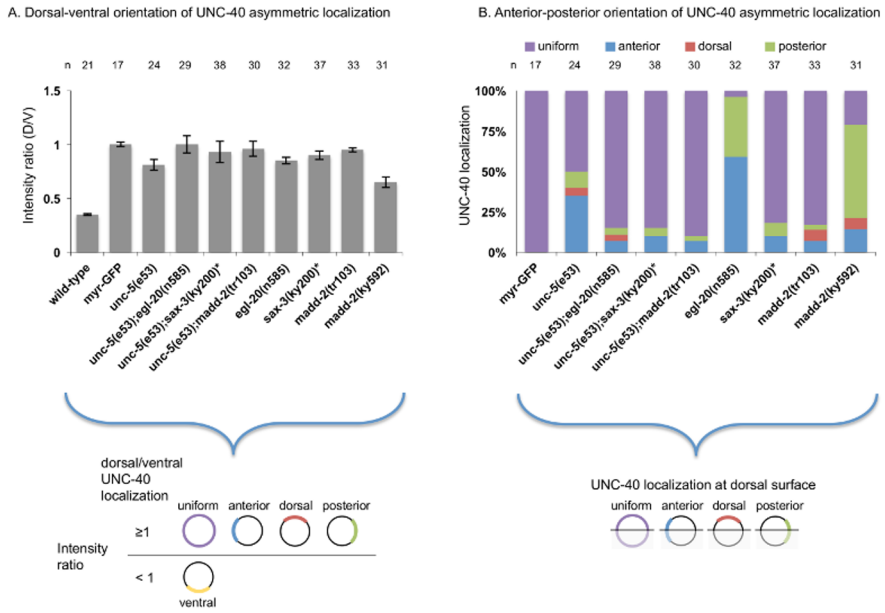

855

856

bioRxiv preprint doi: https://doi.org/10.1101/083436; this version posted October 25, 2016. The copyright holder for this preprint (which was not certified by peer review) is the author/funder, who has granted bioRxiv a license to display the preprint in perpetuity. It is made available under aCC-BY-NC-ND 4.0 International license.

Figure 7. Model for UNC-40 self-organizing polarization and random walk movement. (**A**) Along the plasma membrane, complexes comprising UNC-40 and UNC-5 interact with extracellular cues. A self-organizing process is triggered in which only some complexes emerge to mediate UNC-40 outgrowth activity. In wild-type animals (top) there is a high probability that complexes associated with specific levels of the extracellular cues will mediate outgrowth activity. Compared to wild-type, in animals with loss of UNC-5 function (bottom) the probability of these same complexes mediating outgrowth activity is lower and the probability that the other complexes instead will mediate outgrowth is higher. Direction is labeled left, down, and right, in reference to the orientation of the figure and to emphasize that the model is not referring to any specific cues or their sources in the animal. (**B**) Two sets of tracks are shown to compare random walk models derived from representative wildtype and mutant experimental results. Compared to wildtype, the mutant has a lower probability of outgrowth in one specific direction (down) and a higher probability of outgrowth in other directions (left and right). Using the probability distributions shown below the tracks, 50 simulated random walks of 500 steps were plotted from an origin. This comparison emphasizes that even though the direction of movement is the same, there is a difference in the average displacement. We propose this property of movement is manifested during neuronal extension in wildtype and mutant animals as a difference in the rate of outgrowth. In statistical physics, net movement through the action of random motion is diffusion. Here, each track models the trajectory that mass of the plasma membrane could move during extension. The probability density function of the position of the mass as a function of space and time is described by an advection-diffusion equation. In summary, we suggest that the advection-diffusion model can be used to describe the process by which mass at the leading edge of an extension is transported and that our results describe how genes regulate this transport.

bioRxiv preprint doi: https://doi.org/10.1101/083436; this version posted October 25, 2016. The copyright holder for this preprint (which was not certified by peer review) is the author/funder, who has granted bioRxiv a license to display the preprint in perpetuity. It is made available under aCC-BY-NC-ND 4.0 International license.

882

bioRxiv preprint doi: https://doi.org/10.1101/083436; this version posted October 25, 2016. The copyright holder for this preprint (which was not certified by peer review) is the author/funder, who has granted bioRxiv a license to display the preprint in perpetuity. It is made available under aCC-BY-NC-ND 4.0 International license.

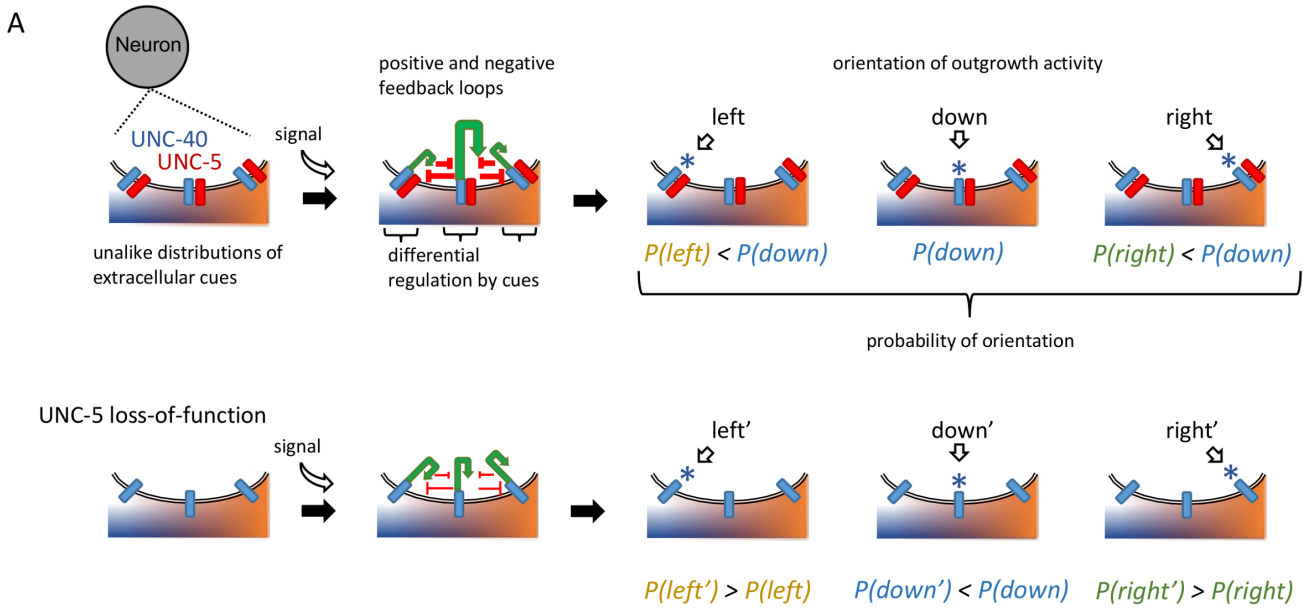

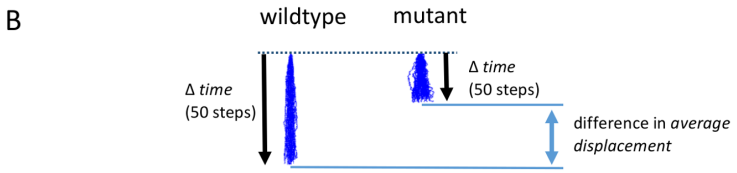

Example:						
	P(right)	=	0.1	0.33	=	*P(right')*
	P(left)	=	0.1	0.33	=	*P(left')*
	P(down)	=	0.8	0.33	=	*P(down')*

883

884

bioRxiv preprint doi: https://doi.org/10.1101/083436; this version posted October 25, 2016. The copyright holder for this preprint (which was not certified by peer review) is the author/funder, who has granted bioRxiv a license to display the preprint in perpetuity. It is made available under aCC-BY-NC-ND 4.0 International license.

885 **Figure 8. Models for how UNC-5 could control the patterns of outgrowth by**
886 **regulating random walk movement.** (**A**) Schematics of the phenotypic differences
887 described in the text. A dashed line connects the schematic to a representative random
888 walk movement model as described in Figure 7B. Our results describe a correlation
889 between the mutant phenotype, which indicates an inhibition of outgrowth, and the random
890 walk modeling, which indicates that the fluctuation in the direction of outgrowth activity
891 observed in the mutant could cause the displacement of the movement of the membrane to
892 decrease. (**B**) An activator-inhibitor model to explain how UNC-5 can regulate the number
893 of processes that can extend in the same direction towards a source of UNC-6. Shown are
894 three panels depicting outgrowth through a gradient of extracellular UNC-6. The UNC-6
895 concentration gradient is depicted by the green color gradient on the right of each panel. In
896 each succeeding panel the leading edge of the extension encounters a higher UNC-6
897 concentration (solid horizontal line). The level of UNC-6 influences UNC-5 signaling, which
898 in turn influences the rate of UNC-40 transport to the plasma membrane surface. UNC-5
899 signaling also results in a decrease in the rate of outgrowth, as depicted by the random walk
900 models below the extension. More specific details about this model are given in the text.
901

bioRxiv preprint doi: https://doi.org/10.1101/083436; this version posted October 25, 2016. The copyright holder for this preprint (which was not certified by peer review) is the author/funder, who has granted bioRxiv a license to display the preprint in perpetuity. It is made available under aCC-BY-NC-ND 4.0 International license.

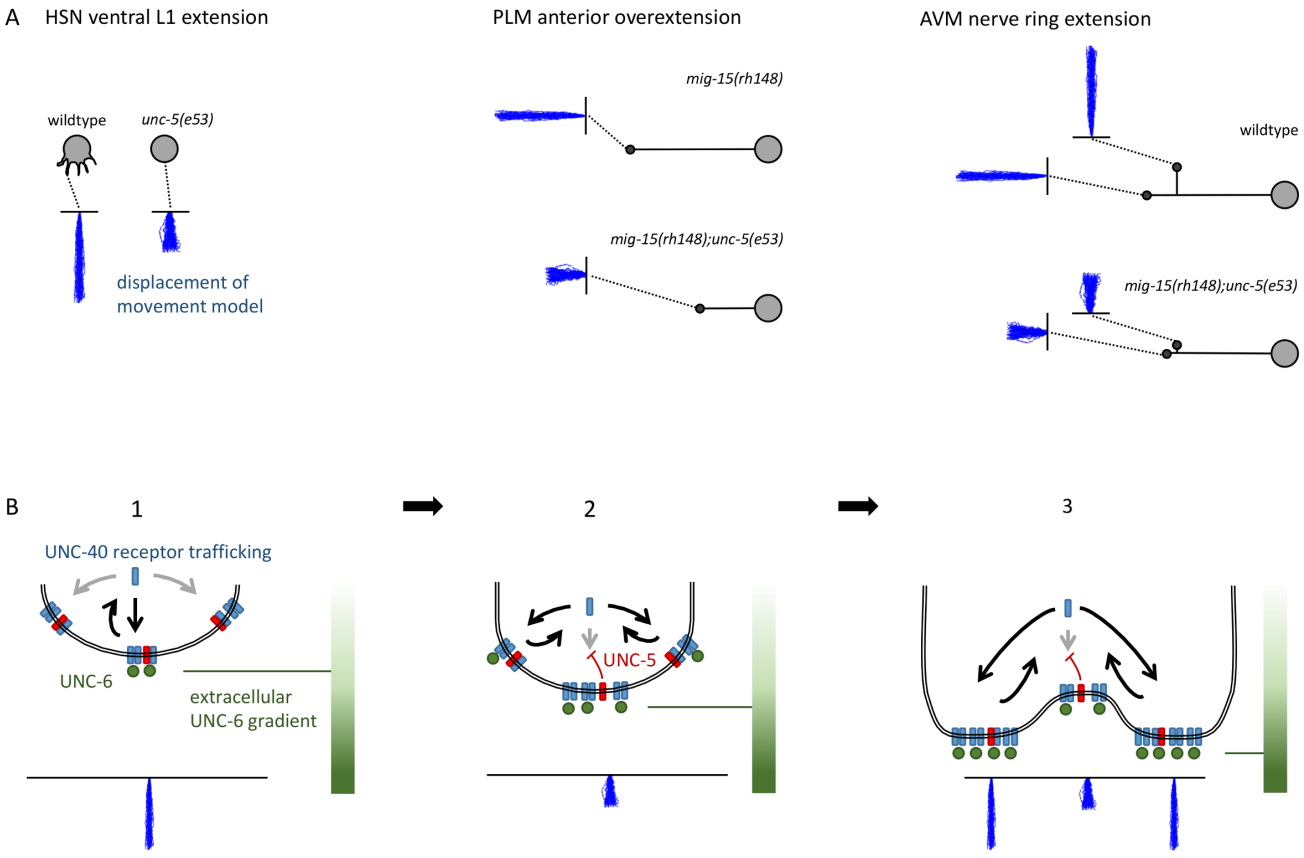

902

903

bioRxiv preprint doi: https://doi.org/10.1101/083436; this version posted October 25, 2016. The copyright holder for this preprint (which was not certified by peer review) is the author/funder, who has granted bioRxiv a license to display the preprint in perpetuity. It is made available under aCC-BY-NC-ND 4.0 International license.

Figure 9. Genetic pathways for self-organizing UNC-40 asymmetric localization. (**A**) Table summarizing the results of experiments previously reported and described in Figure 6 of this paper. (**B**) The genetic data support a model whereby the UNC-6 and EGL-20 extracellular cues regulate at least three pathways leading to robust asymmetric UNC-40 localization. Arrows represent activation; bars represent repression. See text for the logic used to construct the pathways.

bioRxiv preprint doi: https://doi.org/10.1101/083436; this version posted October 25, 2016. The copyright holder for this preprint (which was not certified by peer review) is the author/funder, who has granted bioRxiv a license to display the preprint in perpetuity. It is made available under aCC-BY-NC-ND 4.0 International license.

A

loss-of-function			robust asymmetric UNC-40 localization	reference
unc-6			no	(Kulkarni et al., 2013)
unc-5			yes	(Kulkarni et al., 2013)
unc-5	*unc-6*		no	(Kulkarni et al., 2013)
unc-5	*egl-20*		no	
unc-5	*sax-3*		no	
unc-5	*unc-53*		no	(Kulkarni et al., 2013)
unc-5	*unc-53*	*unc-6*	yes	(Kulkarni et al., 2013)
unc-5	*unc-53*	*sax-3*	no	
unc-5	*madd-2*		no	
unc-6	*unc-53*		yes	(Kulkarni et al., 2013)
unc-6	*sax-3*		no	(Tang and Wadsworth, 2014)
unc-6	*unc-53*	*sax-3*	no	(Tang and Wadsworth, 2014)
egl-20			yes	(Kulkarni et al., 2013)
egl-20	*unc-53*		yes	(Kulkarni et al., 2013)
egl-20	*unc-6*		no	(Kulkarni et al., 2013)
egl-20	*sax-3*		no	(Tang and Wadsworth, 2014)
sax-3			no	(Tang and Wadsworth, 2014)
sax-3	*unc-53*		no	(Tang and Wadsworth, 2014)
unc-53			yes	(Kulkarni et al., 2013)
madd-2			no	
mig-15			yes	(Yang et al., 2014)

B

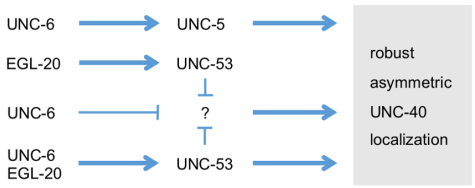

911